
DeTox: Toxic Subspace Projection for Model Editing

Rheeya Uppaal

Department of Computer Sciences
University of Wisconsin-Madison
uppaal@wisc.edu

Apratim Dey

Department of Statistics
Stanford University
apd1995@stanford.edu

Yiting He

Department of Probability and Statistics
University of Science and Technology of China
heyiting@mail.ustc.edu.cn

Yiqiao Zhong

Department of Statistics
University of Wisconsin-Madison
yiqiao.zhong@wisc.edu

Junjie Hu

Department of Computer Sciences and
Department of Biostatistics and Medical Informatics
University of Wisconsin-Madison
jhu@cs.wisc.edu

Abstract

Recent alignment algorithms such as direct preference optimization (DPO) have been developed to improve the safety of large language models (LLMs) by training these models to match human behaviors exemplified by preference data. However, these methods are both computationally intensive and lacking in controllability and transparency, making them prone to jailbreaking and inhibiting their widespread use. Furthermore, these tuning-based methods require large-scale preference data for training and are susceptible to noisy preference data. In this paper, we introduce a tuning-free alignment alternative (DeTox) and demonstrate its effectiveness under the use case of toxicity reduction. Grounded on theory from factor analysis, DeTox is a sample-efficient model editing approach that identifies a toxic subspace in the model parameter space and reduces model toxicity by projecting away the detected subspace. The toxic subspace is identified by extracting preference data embeddings from the language model, and removing non-toxic information from these embeddings. We show that DeTox is more sample-efficient than DPO, further showcasing greater robustness to noisy data. Finally, we establish both theoretical and empirical connections between DeTox and DPO, showing that DeTox can be interpreted as a denoised version of a single DPO step. Our code is available at <https://github.com/Uppaal/detox-edit>.

1 Introduction

The current landscape in NLP is defined by the widespread use of powerful generative large language models (LLMs) with generalist capabilities across domains and tasks. [1–5, *inter alia*]. Their widespread use has shed light on their limitations—they are prone to hallucinations, biases, and generating harmful or toxic text [6–12]. Due to this, ensuring their reliability and safety has become paramount, and is an active area of research known as *alignment* in machine learning.

The core idea is to make a language model match certain human preferred behaviors, like harmlessness, that are exemplified through preference data [3, 13–19, *inter alia*]. Models are trained to learn these

human preferences through algorithms like Proximal Policy Optimization (PPO) [20] or Direct Preference Optimization (DPO) [21]. While promising in many ways [22], models trained through this paradigm may not actually unlearn unwanted behaviors—recent work has shown that these models simply learn stylistic changes in text [23], or redirect activations to avoid toxic regions of the model [24]. Furthermore, curating high-quality preference data and tuning large-scale models are expensive and resource-intensive processes [19, 25, 26], making the process of alignment prohibitive from widespread use.

As a lightweight alternative, model editing [27–36, *inter alia*] is a new and emerging area that attempts to achieve the results of fine-tuning without any gradient-based learning. This is done through performing controlled and targeted interventions on the weights or activations of a model, providing a higher degree of transparency. The Linear Representation Hypothesis [37–42] introduces the idea that various human-interpretable concepts are encoded in linear subspaces of model representations. Leveraging this insight, a vast class of model editing approaches attempt to “push” model activations in directions that encode desired concepts or behaviors. These directions are usually identified through training supervised probes [27, 28], or unsupervised decomposition of activations [29, 30] through singular value decomposition (SVD) [43].

Editing activations in this manner has been shown to successfully make models more truthful [28, 30, 31], moral [30] and unbiased [27, 29, 32–36]. However, one drawback of redirecting activations is that they require additional operations at inference, often leading to architectural changes in the model [28]. In this vein, directly performing edits on weights is more favorable, as this provides a plug-and-play replacement to the original unaligned models.

In this work, we propose a straightforward approach to edit model weights. Focusing on the use-case of toxicity, we introduce DeTox (§4), which identifies toxic directions in model activations to define a low-dimensional toxicity subspace. DeTox then leverages this subspace as a projection filter on the weights, effectively removing these toxic directions from the model and mitigating the model’s toxicity. Our method is based on the heuristic that an embedding vector in any layer of a transformer can be decomposed into interpretable components:

$$\text{embedding vector} \approx \text{high-frequency vector} + \text{toxic vector} + \text{context-dependent vector}$$

Drawing inspiration from classical literature in factor analysis, principal component analysis, and low-rank matrix estimation [44–46], our editing approach effectively decouples these three vector components to isolate and identify the toxic vector, after which it orthogonalizes the weights with respect to the toxic subspace spanned by these toxic vectors. This ensures that during inference, toxic outputs are suppressed. DeTox identifies the subspace associated with toxic factors by applying SVD to embedding differences, effectively canceling out common context factors (§5).

In §7, we empirically validate our method over various models. We demonstrate that our method is highly sample-efficient, requiring orders of magnitude fewer data than alignment algorithms like DPO. Additionally, DeTox is notably robust to labeling noise, outperforming tuning-based alignment algorithms in this regard. Finally, we establish both theoretical (§5) and empirical (§8) connections between DeTox and DPO, showing that our editing approach is conceptually similar to a *denoised* version of a single DPO step.

Our work attempts to provide principled insights toward leveraging interpretable directions in activations for alignment through editing weights. We hope this enables an initial step towards a wider applicability of safe language models.

2 Related Work

Alignment through Training The current standard for aligning models to user-defined preferences is through learning from human [3, 13–16, 18, *inter alia*] or AI [17, 19] feedback via algorithms like PPO [20] or DPO [21]. However, these aligned models have been shown to simply learn stylistic changes [23], or redirect activations to avoid toxic regions of the model [24], leading to easy un-alignment [24, 47, 48] and the possibility of jailbreaking by adversarial prompting [49–55] or fine-tuning [56, 57]. Besides, curating high-quality preference data and tuning large-scale models are expensive and resource-intensive [19, 25, 26], impeding the democratization of aligning models.

	Top Tokens (Layer 14)	Interpretation
μ	, and the - in (" .	Frequent tokens, stopwords
1st svec	s**t f**k ucker b***h slut F**k holes	Toxic tokens
2nd svec	damn really kinda stupid s**t goddamn	Toxic tokens
3rd svec	disclaimer Opinion LĤ Statement Disclaimer Brief	Context dependent topics
4th svec	nation globalization paradigm continent empire ocracy	Context dependent topics

Table 1: Interpreting the top singular vectors of the difference of preference data embeddings. Using GPT-2 and 500 samples from REALTOXICITYPROMPTS, each singular vector of the matrix is interpreted by identifying the top- k tokens it represents. We use the output embedding vector e_j to find top-scoring tokens $j \in \mathcal{V}$ for maximizing $\langle v_i, e_j \rangle$. Tokens have been censored for readability.

Alignment through Editing Activations Model editing involves controlled and targeted interventions on the weights or activations of a model, providing a higher degree of transparency. The Linear Representation Hypothesis [37–42] posits that various human-interpretable concepts are encoded in linear subspaces of model representations. Such directions are typically identified through supervised probes [27, 28, *inter alia*] or unsupervised decompositions of activations [29, 30]. Building upon this, activations have been edited through steering or projecting them on these directions, at inference time or through constrained fine-tuning, to develop models that are more truthful [28, 30, 31], moral [30] and unbiased [27, 29, 32–36].

Alignment through Editing Weights An alternative class of methods applies edits directly on model weights. In comparison to editing activations, these methods serve the advantage of requiring no additional operations at inference, and can be used as plug-and-play replacements to the original models. Recent work studying the key-value store like nature of transformer MLP layers proposed scaling non-toxic components of the weights to reduce model toxicity [58]. A task vector [59–61] is the element-wise sum between a base model and its fine-tuned variant, and encodes the knowledge learnt by the fine-tuned model. These vectors can be manipulated through vector arithmetic to make a model ‘forget’ unwanted behaviors like toxicity [59]. However, their need for models that are fine-tuned on the unwanted behaviour makes the approach computationally expensive.

Most related to our work, a recent study [62] isolated safety critical ranks in the weights of a model through SVD. While we also use low rank decompositions of weights to identify conceptual subspaces, we focus on utilizing these subspaces to remove undesired behaviors from a model in a sample efficient manner. Furthermore, we provide theoretical insights towards why such editing approaches work, and draw connections to tuning based alignment through DPO.

3 Preliminaries

Transformers and MLPs Transformer-based language models map a text sequence into an embedding matrix, which is then passed through multiple transformer layers before the final classification (or output embedding) layer. At each layer ℓ , the self-attention layer encodes a token embedding vector \mathbf{x}_ℓ (for any given position) to $\mathbf{x}_{\ell+0.5}$ which is then passed to the MLP. Recent studies [24, 58, 63, 64, *inter alia*] have shown that MLP layers in language models encode meaningful static concepts, showing that they function analogous to key-value stores. The first MLP ‘key’ layer functions as a pattern detector, while the second ‘value’ layer encodes concepts and information.

Overall, the operation applied by a single transformer layer can be defined as follows,

$$\mathbf{x}_{\ell+1} = \mathbf{x}_{\ell+0.5} + \text{MLP}_\ell(\mathbf{x}_{\ell+0.5}), \quad \text{MLP}_\ell(\mathbf{x}_{\ell+0.5}) = \mathbf{W}_{\ell,V} \sigma(\mathbf{W}_{\ell,K} \mathbf{x}_{\ell+0.5}), \quad (1)$$

where σ is an activation function and $\mathbf{W}_{\ell,K} \in \mathbb{R}^{D_m \times D}$, $\mathbf{W}_{\ell,V} \in \mathbb{R}^{D \times D_m}$ refer to the key and value weights in MLP. We call the i -th row in $\mathbf{W}_{\ell,K}$ and the i -th column in $\mathbf{W}_{\ell,V}$ as the i -th key and value vectors thereafter.

Identifying Concepts by Mapping to Vocabulary To understand what a vector $\mathbf{u} \in \mathbb{R}^D$ in the embedding space represents, a common approach [64] is to use the output embedding matrix¹ $\mathbf{E} = [e_1, \dots, e_{|\mathcal{V}|}]^\top \in \mathbb{R}^{|\mathcal{V}| \times D}$ where \mathcal{V} denotes the vocabulary, and compute a linear map to the

¹In GPT-2, the output embedding matrix is the same as the input token embedding matrix.

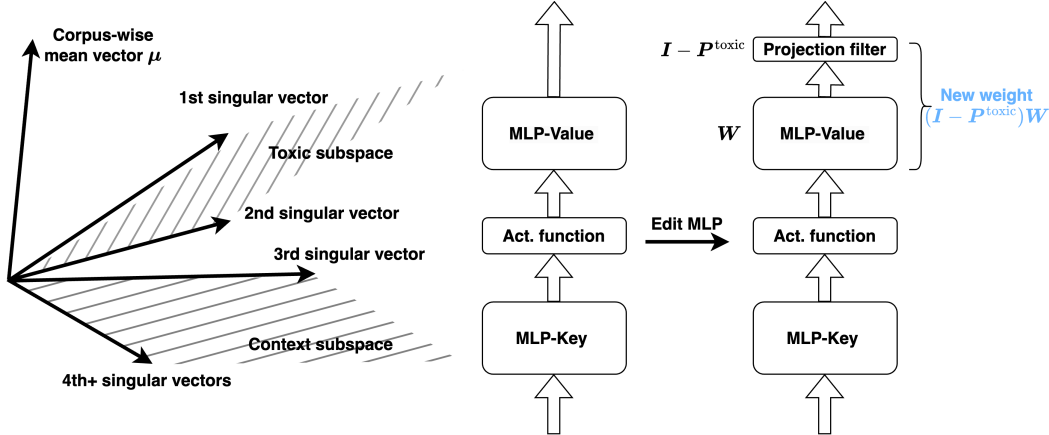


Figure 1: **Left:** Structure of embedding vectors. We posit that a set of singular vectors define the toxic subspace, which is separate from desired model capabilities (such as context subspace and corpus mean direction). **Right:** The DeTox method. We edit the weights of MLP-Value layers through the identification of a projection filter representing the toxic subspace. The edit is performed once, following which the model functions as a drop-in replacement with no architectural modifications.

vocabulary, i.e., $Eu \in \mathbb{R}^{|\mathcal{V}|}$. We then sort Eu in ascending order, find the top- k indices, and use the corresponding tokens to interpret the meaning of u . Intuitively, each output embedding vector e_j gives a similarity score $e_j \cdot u$ that measures how close u and e_j are related, so top scoring tokens explain the meaning of u .

Identifying and Interpreting Toxic Subspaces Building on previous studies that identify directions in the activation space that encode meaningful concepts, we identify a low-dimensional toxicity subspace in the MLP layers of GPT-2. The subspace is identified by computing the difference between activations of toxic and non-toxic data, and obtaining its singular vectors v_1, v_2, \dots through singular value decomposition (SVD). The top singular vectors are inspected by mapping to the vocabulary. In Table 1, we list the top tokens that best explain these singular vectors.

For GPT-2, we discover that v_1, v_2 are mostly associated with toxic words, while v_3 and v_4 likely represent general topics such as news and politics. In addition, we calculate a global mean vector μ , which is associated with frequent tokens and stop words, and is likely to represent corpus-wise frequency statistics. Our interpretations are consistent across different data samples (see §G).

4 DeTox: Editing Weights through Projections on Subspaces

Building on prior work showing that model activation spaces contain interpretable directions, Table 1 suggests that toxicity is encoded in a subspace separating from other directions that encode general concepts (which we call the “context subspace”). To reduce model toxicity, DeTox attempts to identify this toxic subspace and project the model weights out of this subspace. Our approach is described below and summarized in Algorithm 1 (§B).

Formally, given a base model to edit, we assume access to a dataset of toxic and non-toxic sentence pairs $\mathcal{D}_{\text{pref}} = \{(x_i^+, x_i^-)\}_{i=1}^N$. We compute the sentence embeddings of x_i^+, x_i^- , denoted as $\mathbf{x}_{i,\ell}^+, \mathbf{x}_{i,\ell}^-$ respectively at each layer of the language model, $\ell \in \{L_0 \dots L\}$ starting from layer L_0 , and omit the subscript ℓ when context allows (§5). We stack all the sentence embeddings as $\mathbf{X}_\ell^+, \mathbf{X}_\ell^- \in \mathbb{R}^{N \times D}$. Following [29], we identify an approximation of the model’s toxic subspace through the difference of these embeddings:

$$T_\ell^0 := \mathbf{X}_\ell^+ - \mathbf{X}_\ell^- .$$

A key observation suggested by our analysis in Table 1 is that this matrix, while encoding the toxic subspace of the model, also encodes general syntactical and semantic information that must be preserved through the editing process. As a result, we propose a simple three-step algorithm.

Step 1: Filtering Frequent Token Information through Centering We first compute the mean vector $\boldsymbol{\mu} := \text{mean}(\mathbf{X}_\ell^-)$ by averaging across the non-toxic sentence embeddings, which reflects the general statistics of the corpus.² Table 1 shows that $\boldsymbol{\mu}$ likely represents information of stop words that are non-toxic and critical for the model. As a result, we avoid editing weights in the direction of $\boldsymbol{\mu}$ by calculating a centered embedding difference matrix \mathbf{T}_ℓ .

$$\mathbf{T}_\ell := \mathbf{T}_\ell^0 (\mathbf{I} - \mathbf{P}_\mu), \quad \text{where } \mathbf{P}_\mu := \frac{\boldsymbol{\mu}\boldsymbol{\mu}^\top}{\|\boldsymbol{\mu}\|_2^2}. \quad (2)$$

More simply, we project out the component in the direction of $\boldsymbol{\mu}$, so that our further editing (Step 3 below) does not significantly change how the model uses non-toxic frequent tokens.

Step 2: Selecting Toxic Directions To find the dominant directions of the toxic subspace, we apply SVD to \mathbf{T}_ℓ and pick the top- k right singular vectors as the most toxic directions. Subsequently, we define the toxic projection matrix as the sum of the outer product of the toxic singular vectors.

$$\mathbf{U}\boldsymbol{\Sigma}\mathbf{V}^\top = \mathbf{T}_\ell, \quad \mathbf{P}_\ell^{\text{toxic}} := \sum_i^k \mathbf{v}_i \mathbf{v}_i^\top \quad (3)$$

where $\mathbf{v}_1, \mathbf{v}_2, \dots, \mathbf{v}_k$ are the first k column vectors of \mathbf{V} . Table 1 shows interpretations of the singular vectors of \mathbf{V} by mapping them to top similar words in the vocabulary.

Step 3: Projection As the projection matrix $\mathbf{P}_\ell^{\text{toxic}}$ defines the toxic information to be removed from the model, we apply this projection to the original MLP-value weight matrices $\mathbf{W}_{\ell,K}^{\text{original}}$, which are known to encode conceptual information in a model [64]. Finally, the original weight is replaced with the edited weight $\mathbf{W}_{\ell,K}^{\text{edited}}$ in the language model for prediction.

$$\mathbf{W}_{\ell,K}^{\text{edited}} := (\mathbf{I} - \mathbf{P}_\ell^{\text{toxic}}) \mathbf{W}_{\ell,K}^{\text{original}}. \quad (4)$$

5 Theoretical Insights: How DeTox Identifies Toxic Subspaces

A Factor Analysis Perspective Table 1 suggests that the embedding space contains interpretable subspaces. As a result, we use factor analysis, a well-known technique for analyzing such structure. We posit that the sentence embeddings $\mathbf{x}_i^+, \mathbf{x}_i^- \in \mathbb{R}^D$ of a toxic and non-toxic data pair in any given layer (omitting subscript ℓ) follow the factorization:

$$\begin{aligned} \mathbf{x}_i^+ &= \underbrace{a^+ \boldsymbol{\mu}}_{\text{stopwords}} + \underbrace{\mathbf{B}\mathbf{f}_i}_{\text{toxic component}} + \underbrace{\tilde{\mathbf{B}}\tilde{\mathbf{f}}_i}_{\text{context component}} + \underbrace{\mathbf{u}_i^+}_{\text{noise}}, \\ \mathbf{x}_i^- &= a^- \boldsymbol{\mu} + \tilde{\mathbf{B}}\tilde{\mathbf{f}}_i + \mathbf{u}_i^- \end{aligned} \quad (5)$$

where a^+, a^- are scalars of the corpus mean, $\mathbf{B} \in \mathbb{R}^{D \times k}$ contains k ‘‘toxic’’ vectors as its columns, $\tilde{\mathbf{B}} \in \mathbb{R}^{D \times \tilde{k}}$ contains \tilde{k} context vectors as its columns and $\mathbf{f}_i \in \mathbb{R}^k, \tilde{\mathbf{f}}_i \in \mathbb{R}^{\tilde{k}}$ are ‘‘latent factors’’. The toxic subspace is the column space of \mathbf{B} , and a linear combination of its column vectors $\mathbf{B}\mathbf{f}_i$ represents the toxic information in \mathbf{x}_i^+ . We assume both toxic and non-toxic embeddings share a context component. Additionally, there is a noise term representing typical randomness unaccounted for by the statistical model.

Next, we show how DeTox recovers the latent toxic subspace. Recall that $\mathbf{P}_\mu = \boldsymbol{\mu}\boldsymbol{\mu}^\top / \|\boldsymbol{\mu}\|_2^2$. By taking the difference between $\mathbf{x}_i^+, \mathbf{x}_i^-$ and then projecting out the mean direction (that is, multiplying by $\mathbf{I} - \mathbf{P}_\mu$), we have

$$(\mathbf{I} - \mathbf{P}_\mu)(\mathbf{x}_i^+ - \mathbf{x}_i^-) = (\mathbf{I} - \mathbf{P}_\mu)\mathbf{B}\mathbf{f}_i + (\mathbf{I} - \mathbf{P}_\mu)(\mathbf{u}_i^+ - \mathbf{u}_i^-), \quad (6)$$

where $(\mathbf{I} - \mathbf{P}_\mu)\boldsymbol{\mu}(a^+ - a^-) = \mathbf{0}$ since $\mathbf{I} - \mathbf{P}_\mu$ only keeps vectors orthogonal to $\boldsymbol{\mu}$. Let $\mathbf{g}_i := (\mathbf{I} - \mathbf{P}_\mu)(\mathbf{u}_i^+ - \mathbf{u}_i^-)$ and $\mathbf{B}^* := (\mathbf{I} - \mathbf{P}_\mu)\mathbf{B}$. The linear span of \mathbf{B}^* represents the ‘‘centered’’ toxic

²We show in Appendix §B.2 that the mean vector numerically equals the first singular vector of \mathbf{T}_ℓ^0 .

subspace, namely the component of the toxic subspace after removing the corpus-mean component. When DeTox applies SVD to T_ℓ , we can rewrite T_ℓ using B^* as:

$$T_\ell = \underbrace{F(B^*)^\top}_{\text{signal}} + \underbrace{G}_{\text{noise}} = [B^* f_1 + g_1, \dots, B^* f_N + g_N]^\top \in \mathbb{R}^{N \times D} \quad (7)$$

where $F = [f_1, \dots, f_N]^\top$, $G = [g_1, \dots, g_N]^\top$. In the ideal situation $G = \mathbf{0}$ (no noise), the top- k singular vectors span exactly the same subspace of B^* , namely centered toxic subspace. Under nonzero G , SVD is also efficient since SVD gives the best low-rank approximation. Thus, our approach can be viewed as an approximate recovery of the latent subspace for toxic factors.

Denosing with SVD Due to the noise G , we can not recover the centered toxic subspace exactly. Since SVD gives the best low-rank approximation [65], generally we expect to recover the centered toxic subspace $\text{span}(B^*)$ up to some errors. Quantitatively, the recovery error is controlled by the following upper bound where we compare two projection matrices: P^{toxic} from our method, and P_{B^*} associated with the latent subspace.

$$\|P^{\text{toxic}} - P_{B^*}\|_{\text{op}} \leq \frac{C_k \|G\|_{\text{op}}}{\sigma_k(F(B^*)^\top)} \quad (8)$$

where $\|\cdot\|_{\text{op}}$ is the matrix operator norm, C_k is a constant, σ_k returns the k -th singular value of a matrix. Note that the quality of recovering toxic subspace improves as the magnitude of F and B^* increases, which generally happens with a large N and D . See §C for further details.

Connection to DPO DPO [21] is a gradient-based alignment method which is generally nonlinear. To establish a conceptual connection, consider a simple logistic model (π_W) that links hidden states x_i^+ , x_i^- directly to outputs (next-predicted token y_i): the conditional probability is given by

$$\pi_W(y|x_i^+) = Z_W^{-1} \exp(w_y^\top W x_i^+) \quad (9)$$

where w_y is the output embedding vector for any token $y \in \mathcal{V}$, and Z_W is the normalization factor. Similar expression holds if we replace x_i^+ by x_i^- . Some calculation shows that the gradient with respect to W of the DPO loss with one training step is determined by (for a temperature hyperparameter $\beta > 0$)

$$\nabla_W \mathcal{L}_{\text{DPO}}|_{\pi_W = \pi_{\text{ref}}} = -\frac{\beta}{N} \sum_{i=1}^N (w_{y_i^+} (x_i^+)^\top - w_{y_i^-} (x_i^-)^\top). \quad (10)$$

Thus, DPO also finds the toxic subspace approximately by using a variant of embedding differences. Under the factor model assumption in Eq. (5), each row vector behaves as a noise-corrupted vector in the linear span of B and μ , so a large N helps the gradients to “average out” noise due to random sampling. However, it is less sample efficient because SVD directly extracts the low-rank subspace instead of averaging. See §D for further details.

6 Experimental Setup

Models Our main experiments use GPT-2 medium (355M) [66]. Additionally, we use Mistral (7B) [67], its SFT variant Mistral-SFT [68, 18], OPT (6.7B) [69] and GPT-J (6B) [70].

Preference Data We use the pairwise toxic data created by Ref. [24]. The non-toxic sequences are extracted from Wikitext-2 [71], and their toxic counterparts are generated using PPLM [72].

Editing Hyperparameters DeTox involves two hyperparameters: the top- k right singular vectors used to construct the toxic projection matrix P_ℓ^{toxic} , and the layer index to start the edit at L_0 . We use ScreeNot [45] to find an initial estimate for k , and then find an optimal value through cross-validation (§B.1). For GPT-2, $k = 2$ and for all other models $k = 10$. We examine the selection of L_0 in §7, and set $L_0 = 11$ GPT-2 and GPT-J, $L_0 = 15$ for all other models.

Evaluation Following [24], the toxicity of a model is measured by prompting it with the challenge subset of REALTOXICITYPROMPTS [7], which triggers toxic outputs from the language models. We then score the continuations from the model using Detoxify [73], where a higher score indicates a more toxic generation. To ensure the desired model capabilities are not impacted by editing, we measure the perplexity of the model on the dev split of WikiText-2 [71]. Additionally, for larger language models with zero-shot prediction capabilities, we follow [62] and measure the averaged zero-shot capability of the model across seven tasks from EleutherAI LM Harness [74]: BoolQ [75], RTE [76], HellaSwag [77], WinoGrande [78], ARC Easy and Challenge [79], and OpenbookQA [80]. We report the mean and standard deviation of our results over three runs, randomly sampling data.

Comparisons with Tuning-based Alignment: DPO We use the implementation of [24] to train models on the pairwise toxic data using DPO. We use their default hyperparameters and set β to 0.1. For the larger models, we use LoRA [81] on each layer, with a rank of 64, a scaling parameter of 16 and a dropout of 0.1. We use early stopping, i.e., training until the validation loss converges with a patience value of 10.

Model	GPT-2 Medium			Mistral 7B			Mistral-SFT 7B			OPT 6.7B			GPT-J 6B		
Method	Orig	DPO	DeTox	Orig	DPO	DeTox	Orig	DPO	DeTox	Orig	DPO	DeTox	Orig	DPO	DeTox
Toxicity	48.00 (0.00)	36.36 (0.58)	26.83 (0.89)	42.45 (0.00)	36.42 (0.62)	30.40 (0.71)	33.45 (0.00)	23.96 (0.50)	26.03 (1.25)	46.47 (0.00)	45.31 (0.74)	43.49 (1.38)	45.31 (0.00)	43.67 (1.11)	37.36 (2.28)
Perplexity	29.70 (0.00)	29.86 (0.22)	32.50 (0.28)	7.49 (0.00)	7.52 (0.26)	7.99 (0.21)	8.22 (0.00)	8.38 (0.34)	8.83 (0.57)	14.67 (0.00)	14.37 (0.61)	13.83 (0.46)	13.24 (0.00)	13.96 (0.53)	14.53 (0.30)
Capability	-	-	-	64.23	65.32	63.59	63.59	63.66	63.23	51.57	51.55	51.80	51.92	52.46	52.48

Table 2: Comparison of DeTox with DPO. We use $N = 500$ for DeTox and $N = 2000$ for DPO. Despite this, both approaches are comparable in their toxicity reduction, highlighting the sample efficiency of the editing approach. Resulted are averaged over three splits of randomly sampled data.

7 Editing with DeTox is a Robust and Sample Efficient Replacement to DPO

We empirically evaluate our hypothesis by measuring the reduction in toxicity through DeTox relative to DPO. In Table 2, we use 500 datapoints for DeTox and 2,000 datapoints for DPO. Despite this difference in data exposure, DeTox is almost always more effective in reducing toxicity, while still retaining model capability. In Figure 8 (§H), we see that DeTox suppresses the probability of toxic words, relative to the base model (GPT-2). We further highlight the sample efficiency of DeTox in Figure 2 (Table 7 in §H). With no significant detriment to perplexity, the edit approach can reduce toxicity in as little as 5 datapoints, and make significant toxicity reductions with 50 datapoints. In contrast, DPO needs orders of magnitude more data to achieve similar performance.

Editing over Subspaces Elicits Robustness to Labeling Noise Labeling errors when curating data is a pervasive issue towards developing robust models [82–84]. In the setting of toxicity, training on poorly labeled data could result in a *more* toxic model. We test the robustness of DeTox to this, by flipping the labels of a fraction of the dataset. Figure 3 shows that the editing approach, unlike DPO, is almost entirely unaffected by labeling noise, even when half the dataset is incorrectly labeled. This is because the singular vectors of T_ℓ are equivalent to the eigenvectors of Gram matrix $T_\ell^\top T_\ell$, and flipping the sign of any row vector in T_ℓ does not change $T_\ell^\top T_\ell$ at all; see derivation in §B.3.

Centering is Crucial to Retaining Model Capability Each direction in the model embeddings T_ℓ encodes different information, and our method aims to apply edits along the directions that purely encode toxic information. Directions that may partially or totally encode desired knowledge (for example, the context subspace in Figure 1), if included in the edit, can significantly harm model capability. This effect can be seen starkly with the corpus-wide mean μ , which is a direction that encodes basic syntactic knowledge like stop words and frequent tokens (Table 1). This phenomenon is illustrated in Table 3 with GPT-2, using 500 datapoints for editing. Including the corpus mean direction in the edit breaks the model, as evidenced by the model’s high perplexity and nonsensical generations.

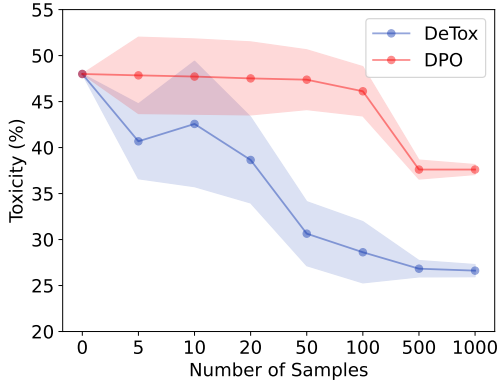


Figure 2: Sample complexity of DeTox and DPO, on GPT-2. DeTox obtains significant toxicity reduction with as few as 50 datapoints, preserving model capability (Table 7). In comparison, DPO requires more data to achieve similar results.

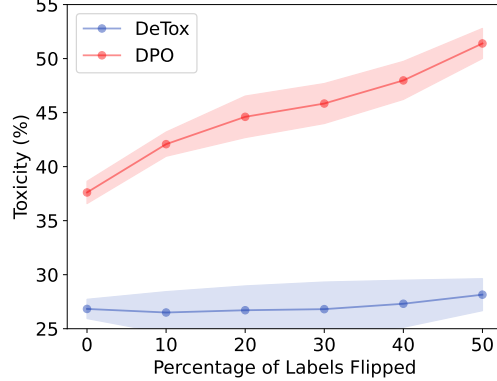


Figure 3: Robustness to label noise, using $N = 500$ on GPT-2. Results with DeTox are marked in blue while DPO are in red. Unlike DPO, DeTox is not impacted by flipping the labels of preference data.

Approach	Toxicity (%)	Perplexity	Generations
Centering	26.83 (0.89)	32.50 (0.28)	The quick brown fox jumps over the lazy dog . Holy School of Medicine, University of California Bloody Cross, the first of the three novels, was
No centering	9.91 (3.50)	94.89 (14.51)	The quick brown fox urchin (Phacronictes alb Holy sh*t, Virginia, June 1, 2017: U Bloody Sunday", "c0", "c0", "c0

Table 3: Impact of centering the preference matrix on edit performance. Skipping the centering, or retaining the corpus mean μ from in the edited knowledge removes basic syntactic knowledge from the model, essentially resulting in nonsensical generations. We use $N = 500$ for editing GPT-2. The generations from the model are shown in blue or red. Toxic words have been censored for readability.

Editing Only Higher Layers Better Preserves Model Capabilities DeTox (Algorithm 1) uses a hyperparameter L_0 that marks the first layer of the model to be edited (i.e., all layers from L_0 to L are edited). Prior work [58, 64] has shown lower layers to process shallow features, while higher layers encode semantic information. For this reason, we always choose L_0 to be one of the middle layers of the model. We justify this choice in Figure 4 (accompanying Table 9), where we show that edits applied on higher layers best reduce toxicity while still preserving model capability.

8 Connections between DeTox and DPO

DeTox Functions as a Denoised Approximation to DPO We examine the question: *Do DPO gradients move the weights in a similar direction as our projection does?* To answer this question, we calculate the DPO gradients \mathbf{G} (at the first training step) with respect to the MLP-value matrix under a varying number of pairwise samples. We then examine the correlation between these DPO gradients and the toxic subspace identified through DeTox. The correlation is defined as the ratio of gradients explained by the toxic subspace, namely $\|\mathbf{P}^{\text{toxic}}\mathbf{G}\|_F / \|\mathbf{G}\|_F$ where $\|\cdot\|_F$ is the Frobenius norm. Figure 5 shows that DPO gradients and $\mathbf{P}^{\text{toxic}}$ are substantially correlated; for comparison, we include a baseline that shows how much $\mathbf{P}^{\text{toxic}}$ explains a random matrix (averaged across 10 independent draws). Further, we find that (1) correlation in later layers is stronger (further justifying the application of the edit on higher layers only), and (2) DPO gradients are explained more with larger sample size. The latter point is consistent with our theoretical insights that DPO needs large samples to “average out” noise.

DPO and DeTox show similar Incremental Layer-wise Contribution Given $L \in \{11, 12, \dots, 24\}$, we are interested in how editing layer 11 through L changes token predictions. We measure the change of token prediction probabilities by applying edits to layer from 11 to L while

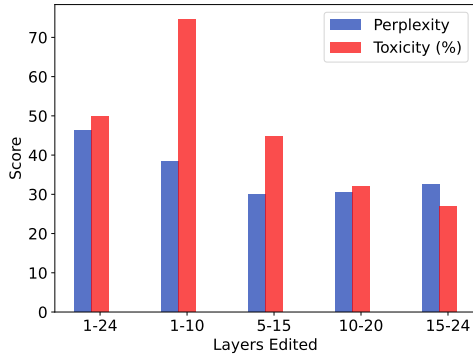


Figure 4: Impact of layer selection on edit performance. Prior studies have shown complex concepts like toxicity to be encoded in higher layers of a model, while lower layers process more basic syntactic and semantic information. Editing the higher layers results in effective toxicity reduction, while preserving perplexity.

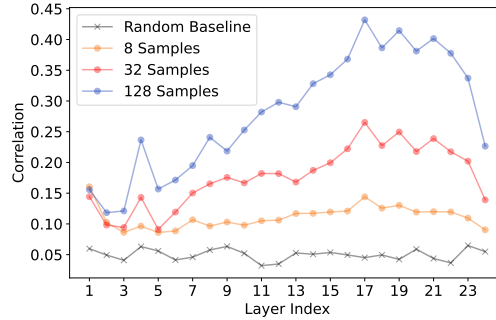


Figure 5: Ratio of DPO gradients explained by toxic subspace: $\|\mathbf{P}^{\text{toxic}}\mathbf{G}\|_F/\|\mathbf{G}\|_F$. The first-step DPO gradients with respect to MLP-value matrix at each layer are calculated under $\{8, 32, 128\}$ samples. For comparison, we report a baseline where the sample ratio with \mathbf{G} is replaced by a random matrix with independent normal random variables.

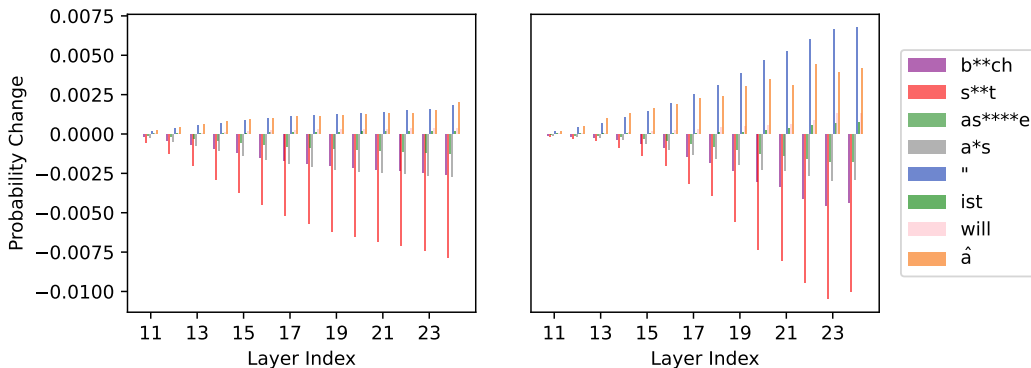


Figure 6: Contribution of Layer 11 through L of alignment models. **Left:** Replacing a base GPT2-medium model with DPO trained at full scaled only for layers 11— L . Probability changes of significantly impacted tokens are plotted against L . **Right:** Apply DeTox only to layers 11— L .

freezing other layers. In Figure 6, we select tokens with most positive/negative changes and plot probability changes against L . We find that DeTox and DPO at full scale exhibit similar patterns: (1) toxic tokens are suppressed after alignment/edit while frequent tokens receive a boost; (2) each subsequent layer contributes incrementally to toxicity reduction, though in DeTox effects are stronger at later layers; (3) moreover, effects of individual layers are nearly *additive*—the combined changes of editing individual layers are nearly the same as editing these layers simultaneously (Appendix I).

9 Limitations and Future Scope

In this work, we introduce DeTox: an interpretable, sample-efficient, and fast weight editing approach for reducing model toxicity. DeTox identifies toxic directions in model activations to define a low-dimensional toxicity subspace. DeTox then leverages this subspace as a projection filter on the weights, effectively removing these toxic directions from the model and mitigating the model’s toxicity. We provide theoretical insights into how DeTox identifies a toxic subspace from a factor analysis perspective and show empirical and theoretical evidence showing that our editing approach is conceptually similar to a *denoised* version of a single DPO step.

DeTox is a powerful sample-efficient alternative to DPO, also showcasing a greater robustness to label noise. However, we note that editing approaches that identify subspaces through unsupervised decomposition of activations are highly sensitive to the selection of singular vectors. Poor selections can result in the desired capabilities of the model being drastically impacted [62].

Extending our work to alignment where the undesired concepts are more subtle (for example, aligning to non-harmful preferences) may prove to be challenging, as subspaces representing these concepts would be more entangled with the context subspaces to be retained. We defer investigating such situations to future work. Finally, our analysis and method focus solely on the MLP layers of the transformer language model. Further explorations into self-attention may help develop more principled and robust edit approaches. We defer this to future work.

Our work attempts to provide principled insights toward leveraging interpretable directions in activations for alignment through editing weights. We hope this enables an initial step toward a wider applicability of modern language models.

Acknowledgement

Uppaal, Zhong, and Hu are supported by the Wisconsin Alumni Research Foundation, and Hu is also supported by the National Institute Of Biomedical Imaging And Bioengineering of the National Institutes of Health under Award Number R01EB033782. The content is solely the responsibility of the authors and does not necessarily represent the official views of the National Institutes of Health.

References

- [1] T. Brown, B. Mann, N. Ryder, M. Subbiah, J. D. Kaplan, P. Dhariwal, A. Neelakantan, P. Shyam, G. Sastry, A. Askell, *et al.*, “Language models are few-shot learners,” *Advances in neural information processing systems*, vol. 33, pp. 1877–1901, 2020.
- [2] T. L. Scao, A. Fan, C. Akiki, E. Pavlick, S. Ilić, D. Hesslow, R. Castagné, A. S. Luccioni, F. Yvon, M. Gallé, *et al.*, “Bloom: A 176b-parameter open-access multilingual language model,” *arXiv preprint arXiv:2211.05100*, 2022.
- [3] H. Touvron, T. Lavril, G. Izacard, X. Martinet, M.-A. Lachaux, T. Lacroix, B. Rozière, N. Goyal, E. Hambro, F. Azhar, *et al.*, “Llama: Open and efficient foundation language models,” *arXiv preprint arXiv:2302.13971*, 2023.
- [4] Y.-S. Chuang, R. Uppaal, Y. Wu, L. Sun, M. N. Sreedhar, S. Yang, T. T. Rogers, and J. Hu, “Evolving domain adaptation of pretrained language models for text classification,” in *NeurIPS 2023 Workshop on Distribution Shifts: New Frontiers with Foundation Models*, 2023.
- [5] R. Uppaal, J. Hu, and Y. Li, “Is fine-tuning needed? pre-trained language models are near perfect for out-of-domain detection,” in *Proceedings of the 61st Annual Meeting of the Association for Computational Linguistics (Volume 1: Long Papers)*, pp. 12813–12832, 2023.
- [6] E. Sheng, K.-W. Chang, P. Natarajan, and N. Peng, “The woman worked as a babysitter: On biases in language generation,” in *Proceedings of the 2019 Conference on Empirical Methods in Natural Language Processing and the 9th International Joint Conference on Natural Language Processing (EMNLP-IJCNLP)*, pp. 3407–3412, 2019.
- [7] S. Gehman, S. Gururangan, M. Sap, Y. Choi, and N. A. Smith, “Realtocixityprompts: Evaluating neural toxic degeneration in language models,” *arXiv preprint arXiv:2009.11462*, 2020.
- [8] R. Bommasani, D. A. Hudson, E. Adeli, R. Altman, S. Arora, S. von Arx, M. S. Bernstein, J. Bohg, A. Bosselut, E. Brunskill, *et al.*, “On the opportunities and risks of foundation models,” *arXiv preprint arXiv:2108.07258*, 2021.
- [9] Z. Kenton, T. Everitt, L. Weidinger, I. Gabriel, V. Mikulik, and G. Irving, “Alignment of language agents,” *arXiv preprint arXiv:2103.14659*, 2021.

- [10] L. Weidinger, J. Mellor, M. Rauh, C. Griffin, J. Uesato, P.-S. Huang, M. Cheng, M. Glaese, B. Balle, A. Kasirzadeh, *et al.*, “Ethical and social risks of harm from language models,” *arXiv preprint arXiv:2112.04359*, 2021.
- [11] A. Toumi and A. Koziell-Pipe, “Functorial language models,” *arXiv preprint arXiv:2103.14411*, 2021.
- [12] Y. Zhang, Y. Li, L. Cui, D. Cai, L. Liu, T. Fu, X. Huang, E. Zhao, Y. Zhang, Y. Chen, *et al.*, “Siren’s song in the ai ocean: a survey on hallucination in large language models,” *arXiv preprint arXiv:2309.01219*, 2023.
- [13] Y. Bai, A. Jones, K. Ndousse, A. Askell, A. Chen, N. DasSarma, D. Drain, S. Fort, D. Ganguli, T. Henighan, *et al.*, “Training a helpful and harmless assistant with reinforcement learning from human feedback,” *arXiv preprint arXiv:2204.05862*, 2022.
- [14] D. M. Ziegler, N. Stiennon, J. Wu, T. B. Brown, A. Radford, D. Amodei, P. Christiano, and G. Irving, “Fine-tuning language models from human preferences,” *arXiv preprint arXiv:1909.08593*, 2019.
- [15] N. Stiennon, L. Ouyang, J. Wu, D. Ziegler, R. Lowe, C. Voss, A. Radford, D. Amodei, and P. F. Christiano, “Learning to summarize with human feedback,” *Advances in Neural Information Processing Systems*, vol. 33, pp. 3008–3021, 2020.
- [16] L. Ouyang, J. Wu, X. Jiang, D. Almeida, C. Wainwright, P. Mishkin, C. Zhang, S. Agarwal, K. Slama, A. Ray, *et al.*, “Training language models to follow instructions with human feedback,” *Advances in neural information processing systems*, vol. 35, pp. 27730–27744, 2022.
- [17] Y. Bai, S. Kadavath, S. Kundu, A. Askell, J. Kernion, A. Jones, A. Chen, A. Goldie, A. Mirhoseini, C. McKinnon, *et al.*, “Constitutional ai: Harmlessness from ai feedback,” *arXiv preprint arXiv:2212.08073*, 2022.
- [18] L. Tunstall, E. Beeching, N. Lambert, N. Rajani, K. Rasul, Y. Belkada, S. Huang, L. von Werra, C. Fourier, N. Habib, *et al.*, “Zephyr: Direct distillation of lm alignment,” *arXiv preprint arXiv:2310.16944*, 2023.
- [19] H. Lee, S. Phatale, H. Mansoor, K. R. Lu, T. Mesnard, J. Ferret, C. Bishop, E. Hall, V. Carbune, and A. Rastogi, “Rlaif: Scaling reinforcement learning from human feedback with ai feedback,” *arXiv preprint arXiv:2309.00267*, 2023.
- [20] J. Schulman, F. Wolski, P. Dhariwal, A. Radford, and O. Klimov, “Proximal policy optimization algorithms,” *arXiv preprint arXiv:1707.06347*, 2017.
- [21] R. Rafailov, A. Sharma, E. Mitchell, S. Ermon, C. D. Manning, and C. Finn, “Direct preference optimization: Your language model is secretly a reward model,” in *ICML 2023 Workshop The Many Facets of Preference-Based Learning*, 2023.
- [22] J. Achiam, S. Adler, S. Agarwal, L. Ahmad, I. Akkaya, F. L. Aleman, D. Almeida, J. Altschmidt, S. Altman, S. Anadkat, *et al.*, “Gpt-4 technical report,” *arXiv preprint arXiv:2303.08774*, 2023.
- [23] B. Y. Lin, A. Ravichander, X. Lu, N. Dziri, M. Sclar, K. Chandu, C. Bhagavatula, and Y. Choi, “The unlocking spell on base llms: Rethinking alignment via in-context learning,” *arXiv preprint arXiv:2312.01552*, 2023.
- [24] A. Lee, X. Bai, I. Pres, M. Wattenberg, J. K. Kummerfeld, and R. Mihalcea, “A mechanistic understanding of alignment algorithms: A case study on dpo and toxicity,” *arXiv preprint arXiv:2401.01967*, 2024.
- [25] E. Strubell, A. Ganesh, and A. McCallum, “Energy and policy considerations for deep learning in nlp,” in *Proceedings of the 57th Annual Meeting of the Association for Computational Linguistics*, pp. 3645–3650, 2019.
- [26] X. Li, Y. Yao, X. Jiang, X. Fang, X. Meng, S. Fan, P. Han, J. Li, L. Du, B. Qin, *et al.*, “Flm-101b: An open llm and how to train it with \$100 k budget,” *arXiv preprint arXiv:2309.03852*, 2023.

- [27] T. Limisiewicz and D. Mareček, “Don’t forget about pronouns: Removing gender bias in language models without losing factual gender information,” in *Proceedings of the 4th Workshop on Gender Bias in Natural Language Processing (GeBNLP)*, pp. 17–29, 2022.
- [28] K. Li, O. Patel, F. Viégas, H. Pfister, and M. Wattenberg, “Inference-time intervention: Eliciting truthful answers from a language model, july 2023,” URL <http://arxiv.org/abs/2306.03341>, 2023.
- [29] S. Bordia and S. R. Bowman, “Identifying and reducing gender bias in word-level language models,” *arXiv preprint arXiv:1904.03035*, 2019.
- [30] A. Zou, L. Phan, S. Chen, J. Campbell, P. Guo, R. Ren, A. Pan, X. Yin, M. Mazeika, A.-K. Dombrowski, *et al.*, “Representation engineering: A top-down approach to ai transparency,” *arXiv preprint arXiv:2310.01405*, 2023.
- [31] J. Campbell, R. Ren, and P. Guo, “Localizing lying in llama: Understanding instructed dishonesty on true-false questions through prompting, probing, and patching,” *arXiv preprint arXiv:2311.15131*, 2023.
- [32] A. Lauscher, G. Glavaš, S. P. Ponzetto, and I. Vulić, “A general framework for implicit and explicit debiasing of distributional word vector spaces,” in *Proceedings of the AAAI Conference on Artificial Intelligence*, vol. 34, pp. 8131–8138, 2020.
- [33] T. Bolukbasi, K.-W. Chang, J. Y. Zou, V. Saligrama, and A. T. Kalai, “Man is to computer programmer as woman is to homemaker? debiasing word embeddings,” *Advances in neural information processing systems*, vol. 29, 2016.
- [34] S. Dev and J. Phillips, “Attenuating bias in word vectors,” in *The 22nd international conference on artificial intelligence and statistics*, pp. 879–887, PMLR, 2019.
- [35] P. O. Aboagye, Y. Zheng, J. Shunn, C.-C. M. Yeh, J. Wang, Z. Zhuang, H. Chen, L. Wang, W. Zhang, and J. Phillips, “Interpretable debiasing of vectorized language representations with iterative orthogonalization,” in *The Eleventh International Conference on Learning Representations*, 2022.
- [36] S. Singh, S. Ravfogel, J. Herzig, R. Aharoni, R. Cotterell, and P. Kumaraguru, “Mimic: Minimally modified counterfactuals in the representation space,” *arXiv preprint arXiv:2402.09631*, 2024.
- [37] K. Park, Y. J. Choe, and V. Veitch, “The linear representation hypothesis and the geometry of large language models,” in *Causal Representation Learning Workshop at NeurIPS 2023*, 2023.
- [38] T. Mikolov, W.-t. Yih, and G. Zweig, “Linguistic regularities in continuous space word representations,” in *Proceedings of the 2013 conference of the north american chapter of the association for computational linguistics: Human language technologies*, pp. 746–751, 2013.
- [39] S. Arora, Y. Li, Y. Liang, T. Ma, and A. Risteski, “A latent variable model approach to pmi-based word embeddings,” *Transactions of the Association for Computational Linguistics*, vol. 4, pp. 385–399, 2016.
- [40] N. Elhage, T. Hume, C. Olsson, N. Schiefer, T. Henighan, S. Kravec, Z. Hatfield-Dodds, R. Lasenby, D. Drain, C. Chen, *et al.*, “Toy models of superposition,” *arXiv preprint arXiv:2209.10652*, 2022.
- [41] Z. Wang, L. Gui, J. Negrea, and V. Veitch, “Concept algebra for (score-based) text-controlled generative models,” *Advances in Neural Information Processing Systems*, vol. 36, 2024.
- [42] N. Nanda, A. Lee, and M. Wattenberg, “Emergent linear representations in world models of self-supervised sequence models,” *arXiv preprint arXiv:2309.00941*, 2023.
- [43] S. Hammarling, “The singular value decomposition in multivariate statistics,” *ACM Sigsum Newsletter*, vol. 20, no. 3, pp. 2–25, 1985.
- [44] H. Abdi and L. J. Williams, “Principal component analysis,” *Wiley interdisciplinary reviews: computational statistics*, vol. 2, no. 4, pp. 433–459, 2010.

- [45] D. Donoho, M. Gavish, and E. Romanov, “Screenot: Exact mse-optimal singular value thresholding in correlated noise,” *The Annals of Statistics*, vol. 51, no. 1, pp. 122–148, 2023.
- [46] J. Fan, K. Wang, Y. Zhong, and Z. Zhu, “Robust high dimensional factor models with applications to statistical machine learning,” *Statistical science: a review journal of the Institute of Mathematical Statistics*, vol. 36, no. 2, p. 303, 2021.
- [47] X. Yang, X. Wang, Q. Zhang, L. Petzold, W. Y. Wang, X. Zhao, and D. Lin, “Shadow alignment: The ease of subverting safely-aligned language models,” *arXiv preprint arXiv:2310.02949*, 2023.
- [48] R. Balestriero, R. Cosentino, and S. Shekkizhar, “Characterizing large language model geometry solves toxicity detection and generation,” *arXiv preprint arXiv:2312.01648*, 2023.
- [49] E. Wallace, S. Feng, N. Kandpal, M. Gardner, and S. Singh, “Universal adversarial triggers for attacking and analyzing nlp,” in *Proceedings of the 2019 Conference on Empirical Methods in Natural Language Processing and the 9th International Joint Conference on Natural Language Processing (EMNLP-IJCNLP)*, pp. 2153–2162, 2019.
- [50] A. Zou, Z. Wang, J. Z. Kolter, and M. Fredrikson, “Universal and transferable adversarial attacks on aligned language models,” *arXiv preprint arXiv:2307.15043*, 2023.
- [51] J. Chu, Y. Liu, Z. Yang, X. Shen, M. Backes, and Y. Zhang, “Comprehensive assessment of jailbreak attacks against llms,” *arXiv preprint arXiv:2402.05668*, 2024.
- [52] X. Shen, Z. Chen, M. Backes, Y. Shen, and Y. Zhang, ““ do anything now”: Characterizing and evaluating in-the-wild jailbreak prompts on large language models,” *arXiv preprint arXiv:2308.03825*, 2023.
- [53] A. Wei, N. Haghtalab, and J. Steinhardt, “Jailbroken: How does llm safety training fail?,” *Advances in Neural Information Processing Systems*, vol. 36, 2024.
- [54] N. Carlini, M. Nasr, C. A. Choquette-Choo, M. Jagielski, I. Gao, P. W. W. Koh, D. Ippolito, F. Tramèr, and L. Schmidt, “Are aligned neural networks adversarially aligned?,” *Advances in Neural Information Processing Systems*, vol. 36, 2024.
- [55] Y. Zeng, H. Lin, J. Zhang, D. Yang, R. Jia, and W. Shi, “How johnny can persuade llms to jailbreak them: Rethinking persuasion to challenge ai safety by humanizing llms,” *arXiv preprint arXiv:2401.06373*, 2024.
- [56] X. Qi, Y. Zeng, T. Xie, P.-Y. Chen, R. Jia, P. Mittal, and P. Henderson, “Fine-tuning aligned language models compromises safety, even when users do not intend to!,” in *The Twelfth International Conference on Learning Representations*, 2023.
- [57] Q. Zhan, R. Fang, R. Bindu, A. Gupta, T. Hashimoto, and D. Kang, “Removing rlhf protections in gpt-4 via fine-tuning,” *arXiv preprint arXiv:2311.05553*, 2023.
- [58] M. Geva, A. Caciularu, K. R. Wang, and Y. Goldberg, “Transformer feed-forward layers build predictions by promoting concepts in the vocabulary space,” *arXiv preprint arXiv:2203.14680*, 2022.
- [59] G. Ilharco, M. T. Ribeiro, M. Wortsman, S. Gururangan, L. Schmidt, H. Hajishirzi, and A. Farhadi, “Editing models with task arithmetic,” *arXiv preprint arXiv:2212.04089*, 2022.
- [60] X. Hu, D. Li, B. Hu, Z. Zheng, Z. Liu, and M. Zhang, “Separate the wheat from the chaff: Model deficiency unlearning via parameter-efficient module operation,” in *Proceedings of the AAAI Conference on Artificial Intelligence*, vol. 38, pp. 18252–18260, 2024.
- [61] L. Gao, Y. Niu, T. Tang, S. Avestimehr, and M. Annavaram, “Ethos: Rectifying language models in orthogonal parameter space,” *arXiv preprint arXiv:2403.08994*, 2024.
- [62] B. Wei, K. Huang, Y. Huang, T. Xie, X. Qi, M. Xia, P. Mittal, M. Wang, and P. Henderson, “Assessing the brittleness of safety alignment via pruning and low-rank modifications,” *arXiv preprint arXiv:2402.05162*, 2024.

- [63] K. Meng, D. Bau, A. Andonian, and Y. Belinkov, “Locating and editing factual associations in gpt,” *Advances in Neural Information Processing Systems*, vol. 35, pp. 17359–17372, 2022.
- [64] M. Geva, R. Schuster, J. Berant, and O. Levy, “Transformer feed-forward layers are key-value memories,” in *Proceedings of the 2021 Conference on Empirical Methods in Natural Language Processing*, pp. 5484–5495, 2021.
- [65] G. H. Golub and C. F. Van Loan, *Matrix computations*. JHU press, 2013.
- [66] A. Radford, J. Wu, R. Child, D. Luan, D. Amodei, I. Sutskever, *et al.*, “Language models are unsupervised multitask learners,” *OpenAI blog*, vol. 1, no. 8, p. 9, 2019.
- [67] A. Jiang, A. Sablayrolles, A. Mensch, C. Bamford, D. Chaplot, D. de las Casas, F. Bressand, G. Lengyel, G. Lample, L. Saulnier, *et al.*, “Mistral 7b (2023),” *arXiv preprint arXiv:2310.06825*, 2023.
- [68] L. Tunstall, E. Beeching, N. Lambert, N. Rajani, S. Huang, K. Rasul, A. M. Rush, and T. Wolf, “The alignment handbook.” <https://github.com/huggingface/alignment-handbook>, 2023.
- [69] S. Zhang, S. Roller, N. Goyal, M. Artetxe, M. Chen, S. Chen, C. Dewan, M. Diab, X. Li, X. V. Lin, *et al.*, “Opt: Open pre-trained transformer language models,” *arXiv preprint arXiv:2205.01068*, 2022.
- [70] B. Wang and A. Komatsuzaki, “Gpt-j-6b: A 6 billion parameter autoregressive language model,” 2021.
- [71] S. Merity, C. Xiong, J. Bradbury, and R. Socher, “Pointer sentinel mixture models,” in *International Conference on Learning Representations*, 2016.
- [72] S. Dathathri, A. Madotto, J. Lan, J. Hung, E. Frank, P. Molino, J. Yosinski, and R. Liu, “Plug and play language models: A simple approach to controlled text generation,” in *International Conference on Learning Representations*, 2019.
- [73] L. Hanu and Unitary team, “Detoxify.” Github. <https://github.com/unitaryai/detoxify>, 2020.
- [74] L. Gao, J. Tow, S. Biderman, S. Black, A. DiPofi, C. Foster, L. Golding, J. Hsu, K. McDonell, N. Muennighoff, *et al.*, “A framework for few-shot language model evaluation,” *Version v0. 0.1. Sept*, p. 8, 2021.
- [75] C. Clark, K. Lee, M.-W. Chang, T. Kwiatkowski, M. Collins, and K. Toutanova, “Boolq: Exploring the surprising difficulty of natural yes/no questions,” in *Proceedings of the 2019 Conference of the North American Chapter of the Association for Computational Linguistics: Human Language Technologies, Volume 1 (Long and Short Papers)*, pp. 2924–2936, 2019.
- [76] A. Wang, A. Singh, J. Michael, F. Hill, O. Levy, and S. Bowman, “Glue: A multi-task benchmark and analysis platform for natural language understanding,” in *Proceedings of the 2018 EMNLP Workshop BlackboxNLP: Analyzing and Interpreting Neural Networks for NLP*, pp. 353–355, 2018.
- [77] R. Zellers, A. Holtzman, Y. Bisk, A. Farhadi, and Y. Choi, “Hellaswag: Can a machine really finish your sentence?,” in *Proceedings of the 57th Annual Meeting of the Association for Computational Linguistics*, pp. 4791–4800, 2019.
- [78] K. Sakaguchi, R. L. Bras, C. Bhagavatula, and Y. Choi, “Winogrande: An adversarial winograd schema challenge at scale,” *Communications of the ACM*, vol. 64, no. 9, pp. 99–106, 2021.
- [79] P. Clark, I. Cowhey, O. Etzioni, T. Khot, A. Sabharwal, C. Schoenick, and O. Tafjord, “Think you have solved question answering? try arc, the ai2 reasoning challenge,” *arXiv preprint arXiv:1803.05457*, 2018.
- [80] T. Mihaylov, P. Clark, T. Khot, and A. Sabharwal, “Can a suit of armor conduct electricity? a new dataset for open book question answering,” in *Proceedings of the 2018 Conference on Empirical Methods in Natural Language Processing*, pp. 2381–2391, 2018.

- [81] E. J. Hu, P. Wallis, Z. Allen-Zhu, Y. Li, S. Wang, L. Wang, W. Chen, *et al.*, “Lora: Low-rank adaptation of large language models,” in *International Conference on Learning Representations*, 2021.
- [82] H.-S. Chang, S. Vembu, S. Mohan, R. Uppaal, and A. McCallum, “Using error decay prediction to overcome practical issues of deep active learning for named entity recognition,” *Machine Learning*, vol. 109, pp. 1749–1778, 2020.
- [83] H. Song, M. Kim, D. Park, Y. Shin, and J.-G. Lee, “Learning from noisy labels with deep neural networks: A survey,” *IEEE transactions on neural networks and learning systems*, 2022.
- [84] D. Chong, J. Hong, and C. D. Manning, “Detecting label errors by using pre-trained language models,” in *Proceedings of the 2022 Conference on Empirical Methods in Natural Language Processing*, pp. 9074–9091, 2022.
- [85] R. B. Cattell, “The scree test for the number of factors,” *Multivariate behavioral research*, vol. 1, no. 2, pp. 245–276, 1966.
- [86] S. Chatterjee, “Matrix estimation by Universal Singular Value Thresholding,” *The Annals of Statistics*, vol. 43, no. 1, pp. 177 – 214, 2015.
- [87] M. Gavish and D. L. Donoho, “The optimal hard threshold for singular values is $4/\sqrt{3}$,” *IEEE Transactions on Information Theory*, vol. 60, no. 8, pp. 5040–5053, 2014.
- [88] D. Donoho and M. Gavish, “Minimax risk of matrix denoising by singular value thresholding,” *arXiv preprint arXiv:1304.2085*, 2014.
- [89] M. Gavish and D. L. Donoho, “Optimal shrinkage of singular values,” *IEEE Transactions on Information Theory*, vol. 63, no. 4, pp. 2137–2152, 2017.
- [90] D. L. Donoho, M. Gavish, and I. M. Johnstone, “Optimal shrinkage of eigenvalues in the spiked covariance model,” *Annals of statistics*, vol. 46, no. 4, p. 1742, 2018.
- [91] C. Davis and W. M. Kahan, “The rotation of eigenvectors by a perturbation. iii,” *SIAM Journal on Numerical Analysis*, vol. 7, no. 1, pp. 1–46, 1970.
- [92] Y. Yu, T. Wang, and R. J. Samworth, “A useful variant of the davis–kahan theorem for statisticians,” *Biometrika*, vol. 102, no. 2, pp. 315–323, 2015.
- [93] P.-Å. Wedin, “Perturbation bounds in connection with singular value decomposition,” *BIT Numerical Mathematics*, vol. 12, pp. 99–111, 1972.
- [94] R. Vershynin, “Introduction to the non-asymptotic analysis of random matrices,” *arXiv preprint arXiv:1011.3027*, 2010.

A Ethical Considerations

Our primary objective is to enhance the safe utility of Large Language Models (LLMs) by reducing the potential harm caused by their outputs. By prioritizing the development of mechanisms to curtail toxicity, we aim to contribute to a more responsible and ethical deployment of LLMs in various applications, thereby safeguarding against the propagation of harmful content and promoting the creation of safer digital environments.

Our study does not involve any human subjects or violation of legal compliance. We do not anticipate any potentially harmful consequences to our work. As detailed in Appendix E, all of our experiments are conducted using publicly available datasets. Our code shall be released for reproducibility. Through our study and releasing our code, we hope to raise stronger research and societal awareness towards building safe and robust language models.

B The DeTox Method

We summarize the DeTox method in Algorithm 1.

Algorithm 1: DeTox Algorithm

Input: Hyperparameter: rank k , starting layer L_0 .
Preference dataset, $\mathcal{D}_{\text{pref}} = \{(x_i^+, x_i^-)\}_{i=1}^N$.
Base model weights, $\mathbf{W}_{\ell, K}$ for all $\ell \in \{L_0 \dots L\}$.
Output: Edited model weights, $\mathbf{W}_{\ell, K}^{\text{edited}}$ for all $\ell \in \{L_0 \dots L\}$

1. **for** $\ell \leftarrow L_0$ to L **do**:
 2. Get hidden sentence embeddings at layer l from $\mathcal{D}_{\text{pref}}$: $\mathbf{X}_\ell^+, \mathbf{X}_\ell^- \in \mathbb{R}^{N \times D}$
 3. Find embedding difference matrix: $\mathbf{T}_\ell^0 \leftarrow (\mathbf{X}_\ell^+ - \mathbf{X}_\ell^-)$
 4. Remove corpus-wise mean vector: $\boldsymbol{\mu} \leftarrow \text{mean}(\mathbf{X}_\ell^-)$ and $\mathbf{T}_\ell \leftarrow \mathbf{T}_\ell^0 (\mathbf{I} - \boldsymbol{\mu}\boldsymbol{\mu}^\top / \|\boldsymbol{\mu}\|_2^2)$
 5. Find toxic subspace projection matrix by SVD: $\mathbf{U}\boldsymbol{\Sigma}\mathbf{V}^\top = \mathbf{T}_\ell, \mathbf{P}_\ell^{\text{toxic}} \leftarrow \sum_{i=1}^k \mathbf{v}_i\mathbf{v}_i^\top$
 6. Edit by projecting away the toxic subspace: $\mathbf{W}_\ell^{\text{edited}} \leftarrow (\mathbf{I} - \mathbf{P}_\ell^{\text{toxic}}) \mathbf{W}_\ell$
 7. **end for**
 8. **return** $\mathbf{W}^{\text{edited}}$
-

B.1 Selection of Top Ranks for Projection Filter

A crucial aspect in factor analysis to tease out the “toxic signal from the noise” is to identify the rank k of the toxic subspace using the preference data. Perhaps the most classical approach is to determine k by the Scree Plot method, also popularly known as the Elbow Method [85]. This method advises us to plot the singular values of the preference data (in descending order of magnitude), find the “elbow”, i.e. the point after which the singular values remain more or less constant, and estimate the rank by the number of singular values larger than the elbow. While extremely popular due to its simplicity, the Scree Plot method is highly subjective, and it is well known that it can be inaccurate in high dimensions. Over the years, a series of works from mathematical statistics has provided principled methods to estimate the rank k in high dimensions, see for example [86–90]. We choose ScreeNot [45] since it provides optimal estimation of the rank under the most minimal assumptions in high dimensions currently known to us. ScreeNot takes as input an upper bound on the rank, which we choose to be 10, as we believe that the toxic information is concentrated in the span of only the top few singular vectors. We applied ScreeNot to the singular values obtained from the preference data per layer obtained from randomly sampled 50 (toxic, non-toxic) sentence pairs, using GPT-2 Medium, LLama and Mistral. We found that the most commonly occurring ranks were 2 and 3, while a few of the ranks were sometimes 4 or 5. It is important to note that ScreeNot optimizes a different loss function, and hence it is not directly suited to provide information about the rank of the toxic subspace. However, ScreeNot aims to find an optimal low rank approximation to the data, and therefore it can be useful to provide tight intervals in which the rank may vary, thereby reducing the size of the grid the experimenter wishes to perform cross validation on, in order to determine the optimal rank suited to their specific problem.

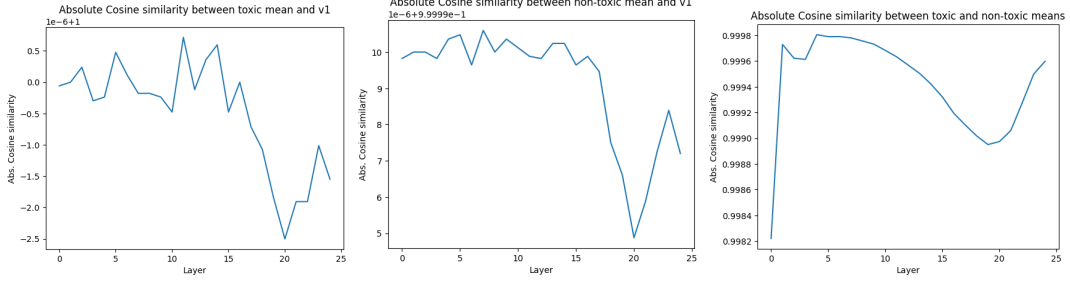


Figure 7: Absolute cosine similarities between the toxic and non-toxic corpus-wide embedding sample means and corresponding top singular vectors per layer. Note the scale in the y-axis. All plots have been obtained using GPT2-medium embeddings applied to $N = 500$ pairs of (toxic, non-toxic) sentences. **Left:** Absolute cosine similarity between the toxic mean vector and top singular vector computed from toxic embeddings. **Middle:** Absolute cosine similarity between the non-toxic mean vector and top singular vector computed from non-toxic embeddings. **Right:** Absolute cosine similarity between the toxic and non-toxic mean vectors.

B.2 Overlap of corpus mean with top singular vector

For each of the collection of toxic and non-toxic sentences, after computing the layer-wise embeddings, we find that the corpus means align significantly with the respective uncentered top singular vectors and also with each other; see Figure 7. In fact, there is almost perfect overlap in all cases. Therefore, in what follows, we will assume that the toxic and non-toxic embeddings share the same mean direction.

B.3 Robustness of DeTox to Label Noise

Here, we provide an explanation why DeTox performs well under label noise. Recall that the singular vectors are given by $U\Sigma V^\top = T_\ell$, where

$$T_\ell = T_\ell^0 (I - \mu\mu^\top / \|\mu\|_2^2)$$

and

$$T_\ell^0 = X_\ell^+ - X_\ell^-$$

Recall our notation $P^{\text{toxic}} = I - \mu\mu^\top / \|\mu\|_2^2$. Denote each row vector of T_ℓ^0 by $t_i \in \mathbb{R}^D$, so $T_\ell^0 = [t_1, \dots, t_N]^\top$.

Label noise in preference data means that the toxic/non-toxic inputs are switched, which results in changing t_i to $-t_i$. The singular vectors V is equivalent to eigenvectors of $T_\ell^\top T_\ell$, and we have

$$\begin{aligned} T_\ell^\top T_\ell &= P^{\text{toxic}} (T_\ell^0)^\top (T_\ell^0) P^{\text{toxic}} \\ &= P^{\text{toxic}} \left(\sum_{i=1}^N t_i (t_i)^\top \right) P^{\text{toxic}}. \end{aligned}$$

From the last expression, it is clear that flipping any t_i to $-t_i$ does not change $T_\ell^\top T_\ell$, thus our method is invariant to label noise.

C Denoising Heuristics

The inequality (8) is due to known results on perturbation of singular subspaces, often known as Davis-Kahan’s theorem [91, 92] and Wedin’s theorem [93]. Let us discuss the implication of this inequality. For simplicity, consider that rank $k = 1$ and each entry of the noise matrix G is independent standard normal random variable. Thus, the inequality (8) implies the following holds with probability at least $1 - 2e^{-N^2}$ [94],

$$\|P^{\text{toxic}} - P_{B^*}\|_{\text{op}} \leq \frac{C(\sqrt{N} + \sqrt{D})}{\|F\|_2 \cdot \|B^*\|_2}$$

where \mathbf{F} and \mathbf{B}^* are vectors of length N and D respectively. Generically, $\|\mathbf{F}\|_2$ scales proportionally to \sqrt{N} and $\|\mathbf{B}^*\|_2$ scales proportionally to \sqrt{D} , so we expect that the upper bound to decrease if we increase either N or D .

D Connections of DeTox to DPO Under a Simple Setting

In this subsection, we exhibit the conceptual connection between DPO [21] and DeTox by studying a simple logistic model for the output token given the (continuing) prompt. In whatever follows, the analysis is performed for each layer ℓ , and to avoid notational burden, we will drop ℓ and focus on each layer separately.

DPO gradient with logistic model For a prompt x with toxic output y^+ and non-toxic output y^- , with corresponding encodings given by $\mathbf{x}, \mathbf{y}^+, \mathbf{y}^-$ respectively, DPO optimizes the loss

$$\mathcal{L}_{\text{DPO}}(\pi_\theta; \pi_{\text{ref}}) = -\mathbb{E}_{(x, y^+, y^-) \sim \mathcal{D}} \left[\log \sigma \left(\beta \log \frac{\pi_\theta(\mathbf{y}^+ | \mathbf{x})}{\pi_{\text{ref}}(\mathbf{y}^+ | \mathbf{x})} - \beta \log \frac{\pi_\theta(\mathbf{y}^- | \mathbf{x})}{\pi_{\text{ref}}(\mathbf{y}^- | \mathbf{x})} \right) \right]$$

where, π_{ref} corresponds to the reference (or base) probability model generating output y given x , π_θ is the new probability model (parametrized by θ), σ is the logistic function with $\sigma(z) = (1 + \exp(-z))^{-1}$, and $\beta > 0$ is a hyperparameter. The gradient of the loss \mathcal{L}_{DPO} with respect to θ at initialization $\pi_\theta = \pi_{\text{ref}}$ equals

$$\nabla_\theta \mathcal{L}_{\text{DPO}}(\pi_\theta; \pi_{\text{ref}}) |_{\pi_\theta = \pi_{\text{ref}}} = -\beta \mathbb{E}_{(x, y^+, y^-) \sim \mathcal{D}} \left[\nabla_\theta \log \pi(\mathbf{y}^+ | \mathbf{x}) - \nabla_\theta \log \pi(\mathbf{y}^- | \mathbf{x}) \right] |_{\pi_\theta = \pi_{\text{ref}}} \quad (11)$$

In the case of language models, let \mathcal{V} denote the vocabulary. We start with a prompt $x \in \mathcal{V}$ and produce M next-token predictions $y_1, \dots, y_M \in \mathcal{V}$ sequentially. Suppose the model sequentially predicts token y_m given $x_m := (x, y_1, \dots, y_{m-1})$ for each $1 \leq m \leq M$, and let \mathbf{x}_m denote the encoding of prompt x_m . We assume a logistic model generating each continuation y_m given x_m , that is,

$$\pi_\theta(y_m | x_m) \equiv \pi_{\mathbf{W}}(y_m | x_m) = Z_{m, \mathbf{W}}^{-1} \exp(\mathbf{w}_{y_m}^\top \mathbf{W} \mathbf{x}_m)$$

Here, \mathbf{w}_{y_m} is the classification vector using which we get prediction y_m given x_m , \mathbf{W} is a weight matrix and $Z_{m, \mathbf{W}}$ is the normalizing constant:

$$Z_{m, \mathbf{W}} = \sum_{y \in \mathcal{V}} \exp(\mathbf{w}_y^\top \mathbf{W} \mathbf{x}_m)$$

We choose to work with the logistic model since modern LLMs (e.g. GPT-2) based on the transformer architecture have the softmax layer, equivalently logistic regression, on top which performs classification to output the next token. We have assumed for simplicity that the classification is performed with linearly transformed prompt encoding $\mathbf{W} \mathbf{x}_m$ instead of the more common non-linear transformations in the transformer architecture. The above model then gives us the joint probability of observing the entire continuation $y = (y_1, \dots, y_M)$ given the starting prompt x as

$$\pi_\theta(y | x) \equiv \pi_{\mathbf{W}}(y | x) = \prod_{m=1}^M \pi_{\mathbf{W}}(y_m | x_m) = Z_{\mathbf{W}}^{-1} \exp\left(\sum_{m=1}^M \mathbf{w}_{y_m}^\top \mathbf{W} \mathbf{x}_m\right)$$

where $Z_{\mathbf{W}} = \prod_{m=1}^M Z_{m, \mathbf{W}}$. We denote by x_m^\pm , \mathbf{x}_m^\pm and $\mathbf{w}_{y_m}^\pm$ the positive/negative continued prompt, the corresponding embedding and classification vector for the positive/negative continuation respectively. Then, plugging this into (11), the first step DPO update has gradient

$$\nabla_{\mathbf{W}} \mathcal{L}_{\text{DPO}}(\pi_{\mathbf{W}}; \pi_{\text{ref}}) |_{\pi_{\mathbf{W}} = \pi_{\text{ref}}} = -\beta \mathbb{E}_{(x, y^+, y^-) \sim \mathcal{D}} \left[\sum_{m=1}^M (\mathbf{w}_{y_m^+}^\top (\mathbf{x}_m^+)^\top - \mathbf{w}_{y_m^-}^\top (\mathbf{x}_m^-)^\top) \right]$$

Note that the the normalization factors $Z_{m, \mathbf{W}}$ (and hence $Z_{\mathbf{W}}$) are cancelled out when we take the difference of the gradients of the log-probabilities. With N pairs of (toxic, non-toxic) prompts in the dataset \mathcal{D} , the first step DPO gradient will be an average over all the pairs:

$$\nabla_{\mathbf{W}} \mathcal{L}_{\text{DPO}}(\pi_{\mathbf{W}}; \pi_{\text{ref}}) |_{\pi_{\mathbf{W}} = \pi_{\text{ref}}} = -\frac{\beta}{N} \sum_{i=1}^N \sum_{m=1}^M (\mathbf{w}_{y_{i,m}^+}^\top (\mathbf{x}_{i,m}^+)^\top - \mathbf{w}_{y_{i,m}^-}^\top (\mathbf{x}_{i,m}^-)^\top)$$

where the extra index i in the subscript of $y_{i,m}, \mathbf{x}_{i,m}$ simply corresponds to y_m, \mathbf{x}_m for i 'th prompt in the corpus.

We consider the case $M = 1$ for simplicity; the forthcoming derivations extend to the general case $M > 1$ by some notational book-keeping. Dropping M from the notation, the first step DPO gradient equals

$$\nabla_{\mathbf{W}} \mathcal{L}_{\text{DPO}}(\pi_{\mathbf{W}}; \pi_{\text{ref}})|_{\pi_{\mathbf{W}}=\pi_{\text{ref}}} = -\frac{\beta}{N} \sum_{i=1}^N (\mathbf{w}_{y_i}^+(\mathbf{x}_i^+)^\top - \mathbf{w}_{y_i}^-(\mathbf{x}_i^-)^\top)$$

As mentioned in Section 5, we use the factor model for each sentence embedding:

$$\begin{aligned} \mathbf{x}_i^+ &= \underbrace{a^+ \boldsymbol{\mu}}_{\text{stopwords}} + \underbrace{\mathbf{B} \mathbf{f}_i}_{\text{toxic component}} + \underbrace{\tilde{\mathbf{B}} \tilde{\mathbf{f}}_i}_{\text{context component}} + \underbrace{\mathbf{u}_i^+}_{\text{noise}}, \\ \mathbf{x}_i^- &= a^- \boldsymbol{\mu} + \tilde{\mathbf{B}} \tilde{\mathbf{f}}_i + \mathbf{u}_i^- \end{aligned} \quad (12)$$

where, recall, a^+, a^- are scalars, $\mathbf{B} \in \mathbb{R}^{D \times r}$, $\tilde{\mathbf{B}} \in \mathbb{R}^{D \times \tilde{r}}$ and $\mathbf{f}_i \in \mathbb{R}^r$, $\tilde{\mathbf{f}}_i \in \mathbb{R}^{\tilde{r}}$. The reason why we can use the same mean direction $\boldsymbol{\mu}$ is justified by our discussion in §B.2. Thus, the contribution of pair i to the gradient is

$$\begin{aligned} \mathbf{w}_{y_i}^+(\mathbf{x}_i^+)^\top - \mathbf{w}_{y_i}^-(\mathbf{x}_i^-)^\top &= (a^+ \mathbf{w}_{y_i}^+ - a^- \mathbf{w}_{y_i}^-) \boldsymbol{\mu}^\top + \mathbf{w}_{y_i}^+(\mathbf{f}_i^+)^\top \mathbf{B}^\top \\ &\quad + (\mathbf{w}_{y_i}^+ - \mathbf{w}_{y_i}^-) \tilde{\mathbf{f}}_i^\top \tilde{\mathbf{B}}^\top + (\mathbf{w}_{y_i}^+(\mathbf{u}_i^+)^\top - \mathbf{w}_{y_i}^-(\mathbf{u}_i^-)^\top) \end{aligned}$$

The full gradient is given by the average of these quantities. We observe that this gradient involves \mathbf{B} along with $\boldsymbol{\mu}$ and noise, and hence may be interpreted as containing noisy information about \mathbf{B} . As a result, DPO first step gradient update can be interpreted as a *noisy* elimination of toxic information contained in \mathbf{B} from \mathbf{W} .

This inspires the following thought: if one can estimate \mathbf{B} better, it may be possible to eliminate the effect of \mathbf{B} in a more pronounced way from \mathbf{W} . In a sense, this would be akin to performing a *denoised* DPO first step gradient update. To extract information on \mathbf{B} , we consider the pairwise differences of the sentence embeddings, which translates into looking at the matrix of encoding differences

$$\mathbf{T}^0 = \mathbf{X}^+ - \mathbf{X}^-$$

where \mathbf{X}^+ and \mathbf{X}^- contain the toxic and non-toxic embeddings $\mathbf{x}_i^+, \mathbf{x}_i^-$ as the rows. As discussed in Section 5, we perform SVD on \mathbf{T}^0 , project out the first principal component direction (to eliminate the effect of $\boldsymbol{\mu}$) and consider the first k components after that spanning our toxicity subspace. As a result, we can identify $\mathbf{P}_{\mathbf{B}}$ as the subspace spanned by the toxic vectors, and hence eliminate $\mathbf{P}_{\mathbf{B}}(\mathbf{W})$ from \mathbf{W} , which is equivalent to performing $(\mathbf{I} - \mathbf{P}_{\mathbf{B}})(\mathbf{W})$, and this is exactly our proposed edit method.

E Datasets

To reduce model toxicity, we use the pairwise toxic data generated by [24]. The dataset is created using sequences from Wikitext-2 [71]. For each non-toxic sequence, a toxic variant is generated using PPLM [72].

The evaluation of model toxicity is done by prompting the model on prompts from the challenge subset of the REALTOXICITYPROMPTS [7] dataset. These prompts are known to elicit highly toxic continuations from models.

Model capability is evaluated through perplexity on the dev split of the WikiText-2-v1 dataset [71]. Additionally, for larger language models with zero-shot prediction capabilities, we follow [62] and measure the averaged zero-shot capability of the model across the dev or test splits of seven tasks from EleutherAI LM Harness [74]: BoolQ [75], RTE [76], HellaSwag [77], WinoGrande [78], ARC Easy and Challenge [79], and OpenbookQA [80].

More details on these datasets can be found in Table 4.

Dataset	Language	License	Number of Samples
DPO-Toxic [24]	English	MIT	24,576
RealToxicityPrompts (Challenge) [7]	English	Apache	1199
WikiText-2 [71]	English	CC BY-SA 4.0	2064
BoolQ [75]	English	CC BY-SA 3.0	3270
RTE [76]	English	Unknown	3000
HellaSwag [77]	English	MIT	10003
Winogrande [78]	English	Unknown	1767
ARC [79]	English	Unknown	3548
OpenbookQA [80]	English	Unknown	500

Table 4: Artifacts used in our study. The dataset statistics report the values used in our study.

F Implementation Details

Models and Implementation We use GPT-2³ [66], Mistral⁴ [67], Mistral-SFT⁵, OPT⁶ [69] and GPT-J⁷ [70] from the HuggingFace library⁸, and use PyTorch⁹ to edit our models. We use the codebase of [24]¹⁰ for training DPO models.

Edit Details We use $N = 500$ datapoints for editing with DeTox. For GPT-2, we set the rank hyperparameter $k = 2$ and edit layers 15-24. For all other models, we use $k = 10$ and edit layers 20-32 (for GPT-J, we edit layers 10-28). All results are averaged over three runs, with different random subsets of data used. We report the mean and standard deviation across these runs.

Training We use the implementation of [24] to train models on the pairwise toxicity data using DPO. We use their default hyperparameters, and set β to 0.1. For the 7B size models, we use LoRA [81] on each layer, with a rank of 64, scaling parameter of 16 and dropout of 0.1. We use early stopping, training until the validation loss converges with a patience value of 10.

Computations The DeTox weight editing method is designed to be highly compute inefficient, requiring a small number of samples to achieve strong performance. Furthermore, the approach is tuning free and requires only one forward pass from the model. Table 5 compares the time and memory costs of DeTox and DPO on a single NVIDIA RTX A6000 GPU. In total, we run 150 experiments (DeTox and DPO combined) across all models. Excluding evaluation time, our total compute period is approximately 9 GPU hours.

Method	Time (seconds)	System Memory (MB)	GPU Memory (MB)
DeTox	16.26	6767.16	9614.00
DPO	187.15	3471.23	10019.00

Table 5: Comparison of computational costs. Using $N = 500$ with GPT-2 medium on one NVIDIA RTX A6000 GPU, DeTox is significantly faster than DPO.

G Additional Results for Interpreting Singular Vectors

In Table 6, we use DeTox and interpret the singular vectors using the same map to vocabulary approach as in Table 1 but on a different chunk of data from REALTOXICITYPROMPTS.

³<https://huggingface.co/openai-community/gpt2-medium>

⁴<https://huggingface.co/mistralai/Mistral-7B-v0.1>

⁵<https://huggingface.co/HuggingFaceH4/mistral-7b-sft-beta>

⁶<https://huggingface.co/facebook/opt-6.7b>

⁷<https://huggingface.co/EleutherAI/gpt-j-6b>

⁸<https://github.com/huggingface/transformers>

⁹<https://pytorch.org/>

¹⁰https://github.com/ajyl/dpo_toxic

	Top Tokens (Layer 14)	Interpretation
μ	, and the - in a (" .	Frequent tokens, stopwords
1st svec	s**t f**k b**ch slut ucker F**k holes sucker	Toxic tokens
2nd svec	damn really kinda f**king s**t messed REALLY somebody	Toxic tokens
3rd svec	Opinion understatement disclaimer Editors "]=> Regarding Statement	Context dependent topics
4th svec	ideals religions ideologies philosophies democracies	Context dependent topics

Table 6: Interpretability is robust: similar to Table 1 but based on a different batch of 500 samples from the same dataset.

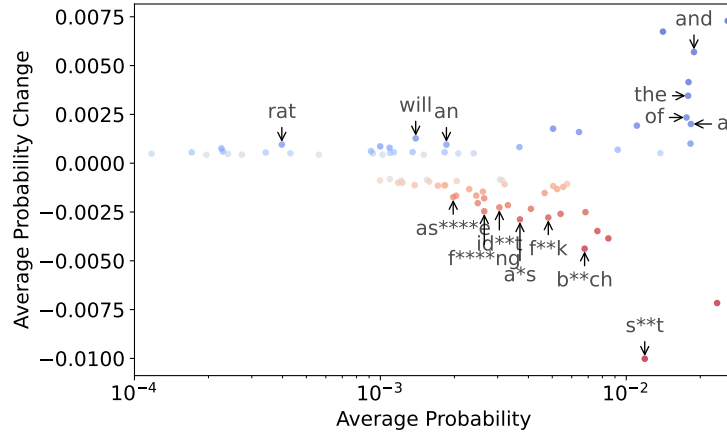


Figure 8: Relationship between average prediction probability and average probability change for tokens with the most probability change. The x -axis represents the average prediction probability of each token across 500 samples using GPT-2 medium, while the y -axis denotes their average prediction probability change after using DeTox.

H Evaluating the Utility of DeTox

The DeTox method works as an effective and sample efficient replacement to DPO for reducing toxicity. In Figure 8, we see that DeTox reduces the probability of toxic words, relative to the base model (GPT-2).

DeTox is Robust to Sample Selection DeTox is unaffected by the selection of samples. We calculate the correlation between $\mathbf{P}^{\text{toxic}}$ extracted from various runs. We use the $\mathbf{P}^{\text{toxic}}$ from one run of $N = 500$ as our control, and calculate its correlation with two other runs with $N = 50$ and 500 respectively. Correlation is computed as the norm of the projection: $\|\mathbf{P}^{\text{toxic}} \mathbf{P}_{\text{control}}^{\text{toxic}}\|_F / \|\mathbf{P}_{\text{control}}^{\text{toxic}}\|_F$. In Figure 9, we see that both variants of $\mathbf{P}^{\text{toxic}}$ have very high correlation with the control. Furthermore, a random gaussian matrix with the same moments as the control has nearly no correlation.

Sample Complexity Table 7 accompanies Figure 2 (§7) and shows a comparison of DeTox and DPO in sample complexity. While DPO requires large amounts of data to make significant reductions in toxicity, DeTox achieves the same in as little as 50 samples.

Robustness to Label Noise Table 8 accompanies Figure 3 (§7) and compares the impact of label flipping noise on DPO and DeTox. As the degree of noise increases, DPO understandably increases model toxicity. However, DeTox is not impacted by such noise, and toxicity reductions remain similar.

Impact of Editing across Layers Table 9 accompanies Figure 4 (§7), showing the impact of layer selection for editing on toxicity reduction. We see that edits on higher layers preserve model perplexity while also reducing toxicity.

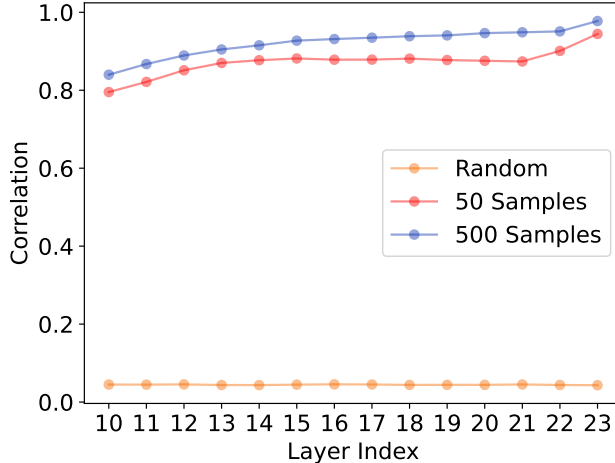


Figure 9: DeTox is robust to the selection of samples. We compare the correlation between We calculate the correlation between P^{toxic} extracted from various runs. We use the P^{toxic} from one run of $N = 500$ as our control, and calculate its correlation with two other runs with $N = 50$ and 500 respectively. Both variants of P^{toxic} have very high correlation with the control. Furthermore, a random gaussian matrix with the same moments as the control has nearly no correlation.

Datapoints	DPO		DeTox	
	Toxicity(%)	Perplexity	Toxicity(%)	Perplexity
0	48.00 (0.00)	29.70 (0.00)	48.00 (0.00)	29.70 (0.00)
5	47.85 (4.15)	29.71 (0.63)	40.68 (4.07)	31.19 (0.51)
10	47.72 (4.09)	29.70 (0.37)	42.57 (6.82)	31.20 (0.42)
20	47.52 (3.97)	29.70 (0.22)	38.65 (4.67)	31.95 (0.68)
50	47.38 (3.25)	29.75 (0.45)	30.64 (3.48)	31.37 (0.42)
100	46.12 (2.68)	29.69 (0.43)	28.62 (3.33)	32.37 (0.28)
500	37.61 (1.03)	29.78 (0.21)	26.83 (0.89)	32.50 (0.28)
1000	37.61 (0.54)	29.78 (0.18)	26.62 (0.66)	32.26 (0.13)

Table 7: Sample complexity of DeTox and DPO, on GPT-2 medium. DeTox obtains significant toxicity reduction with as few as 50 datapoints, unlike DPO which needs orders of magnitude more data to achieve similar performance.

LLM Utility Evaluation In Table 2 (§7), we compare DeTox and DPO across different models, reporting the model capability as its averaged zero-shot capability of the model across seven tasks from EleutherAI LM Harness [74]: BoolQ [75], RTE [76], HellaSwag [77], WinoGrande [78], ARC Easy and Challenge [79], and OpenbookQA [80]. Tables 10, 11, 12 and 13 report the task wise performance for all models in our experiments.

I Layer Attribution Analysis

We present evidence using GPT2-medium that individual aligned/edited layer has an additive effects to toxicity alignment.

For DeTox, we first editing layer 11 through L as considered in Section 8 and calculate changes in prediction probabilities denoted by $r_{11:L}(t)$ for any token t . Then, we apply our edit at layer $L \in \{11, 12, \dots, 24\}$ one at a time and calculate the probability change, denoted by $r_L(t)$ for any token t . For DPO, we make similar calculations: first using multiple DPO layers to replace the layers from the base model, and then using individual DPO layer.

We plot two curves for both DeTox and DPO trained at full scale.

- Solid curve: $r_{11:L}(t)$ plotted against L for significantly impacted tokens t .

Flipped Samples(%)	DPO		DeTox	
	Toxicity(%)	Perplexity	Toxicity(%)	Perplexity
0	37.61 (1.03)	29.78 (0.21)	26.83 (0.89)	32.50 (0.28)
10	42.08 (0.72)	29.58 (0.27)	26.50 (1.93)	32.19 (0.14)
20	44.61 (0.84)	29.70 (0.16)	26.71 (2.25)	32.14 (0.18)
30	45.84 (0.60)	29.73 (0.25)	26.81 (2.51)	32.06 (0.30)
40	47.98 (0.47)	29.84 (0.29)	27.31 (2.18)	31.97 (0.41)
50	51.40 (0.56)	29.95 (0.28)	28.15 (1.48)	31.96 (0.38)

Table 8: Robustness to label noise, using $N = 500$ on GPT-2. Unlike DPO, DeTox is not impacted by flipping the labels of preference data. This is because the singular vectors of the toxic subspace, generated through SVD, do not have unique signs.

Layers Edited	Toxicity (%)	Perplexity
1-24	49.80 (1.10)	46.25 (5.99)
1-10	74.63 (9.61)	38.41 (2.47)
5-15	44.81 (1.97)	30.06 (0.18)
10-20	32.04 (1.57)	30.37 (0.19)
15-24	26.83 (0.89)	32.50 (0.28)

Table 9: Impact of layer selection on edit performance. Prior studies have shown complex concepts like toxicity to be encoded in higher layers of a model, while lower layers process more basic syntactic and semantic information. Editing the higher layers results in effective toxicity reduction, while preserving perplexity.

Dataset	Method		
	Original	DPO	DeTox
BoolQ	83.76 (0.65)	83.55 (0.65)	81.80 (0.67)
RTE	67.15 (2.83)	67.15 (2.83)	64.62 (2.88)
HellaSwag	61.29 (0.49)	61.70 (0.49)	61.76 (0.48)
WinoGrande	73.95 (1.23)	74.03 (1.23)	70.96 (1.28)
ARC Easy	80.89 (0.81)	81.31 (0.80)	80.68 (0.81)
ARC Challenge	50.17 (1.46)	51.11 (1.46)	51.02 (1.46)
OpenbookQA	32.40 (2.10)	33.00 (2.10)	31.40 (2.08)
Average	64.23	65.32	63.59

Table 10: Model capability of Mistral (7B), as measured through zero-shot performance on seven tasks of ElutherAI LM Harness. Capability is not significantly affected by DPO or DeTox.

Dataset	Method		
	Original	DPO	DeTox
BoolQ	85.08 (0.62)	85.32 (0.62)	84.53 (0.63)
RTE	63.90 (2.89)	63.90 (2.89)	62.09 (2.92)
HellaSwag	61.04 (0.49)	61.25 (0.49)	62.32 (0.48)
WinoGrande	72.53 (1.25)	71.67 (1.27)	71.11 (1.27)
ARC Easy	81.02 (0.80)	81.27 (0.80)	80.18 (0.82)
ARC Challenge	51.37 (1.46)	51.79 (1.46)	51.88 (1.46)
OpenbookQA	30.20 (2.06)	30.40 (2.06)	30.40 (2.06)
Average	63.59	63.66	63.23

Table 11: Model capability of Mistral-SFT (7B), as measured through zero-shot performance on seven tasks of ElutherAI LM Harness. Capability is not significantly affected by DPO or DeTox.

Dataset	Original	Method DPO	DeTox
BoolQ	66.02 (0.83)	66.21 (0.83)	64.68 (0.84)
RTE	55.23 (2.99)	55.23 (2.99)	57.40 (2.98)
HellaSwag	50.51 (0.50)	50.50 (0.50)	50.69 (0.50)
WinoGrande	65.35 (1.34)	65.04 (1.34)	65.35 (1.34)
ARC Easy	65.66 (0.97)	65.82 (0.97)	65.45 (0.98)
ARC Challenge	30.63 (1.35)	30.63 (1.35)	31.06 (1.35)
OpenbookQA	27.60 (2.00)	27.40 (02.00)	28.00 (2.01)
Average	51.57	51.55	51.80

Table 12: Model capability of OPT (6.7B), as measured through zero-shot performance on seven tasks of ElutherAI LM Harness. Capability is not significantly affected by DPO or DeTox.

Dataset	Original	Method DPO	DeTox
BoolQ	0.6544 (0.0083)	0.6492 (0.0083)	0.6367 (0.0084)
RTE	0.5451 (0.0300)	0.5704 (0.0298)	0.5379 (0.030)
HellaSwag	0.4953 (0.0050)	0.5001 (0.0050)	0.5120 (0.0050)
WinoGrande	0.6409 (0.0135)	0.6401 (0.0135)	0.6346 (0.0135)
ARC Easy	0.6692 (0.0097)	0.6755 (0.0096)	0.6738 (0.0096)
ARC Challenge	0.3396 (0.0138)	0.3490 (0.0139)	0.3524 (0.0140)
OpenbookQA	0.2900 (0.0203)	0.2880 (0.0203)	0.3260 (0.0210)
Average	51.92	52.46	52.48

Table 13: Model capability of GPT-J (6B), as measured through zero-shot performance on seven tasks of ElutherAI LM Harness. Capability is not significantly affected by DPO or DeTox.

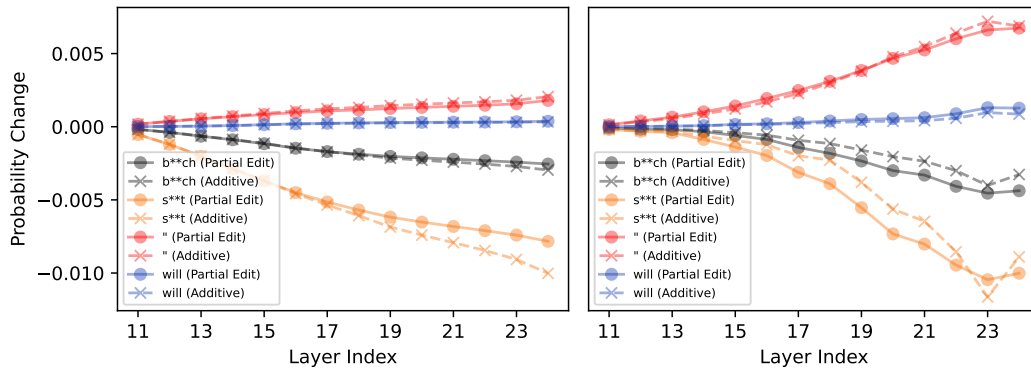


Figure 10: **Additivity check.** **Left:** Replacing the base model with DPO layers from 11 to L simultaneously (solid) vs. replacing each layer one at a time and then summing the individual effects (dashed). **Right:** Editing layers from 11 to L using DeTox simultaneously vs. editing each layer one at a time and then summing the individual effects.

- Dashed curve: $\sum_{j=11}^L r_j(t)$ plotted against L for significantly impacted tokens t .

Thus, solid curve represents block effects where multiple adjacent layers are edited simultaneously while dashed curve represents individual effects.

We find that the solid curve and the dashed curve in both plots are mostly aligned. This suggests that the effects of layers in terms of probability changes are nearly additive, i.e., $r_{11:L}(t) \approx \sum_{j=11}^L r_j(t)$.

J NeurIPS Paper Checklist

Claims *Do the main claims made in the abstract and introduction accurately reflect the paper’s contributions and scope? Claims in the paper should match theoretical and experimental results in terms of how much the results can be expected to generalize. The paper’s contributions should be clearly stated in the abstract and introduction, along with any important assumptions and limitations. It is fine to include aspirational goals as motivation as long as it is clear that these goals are not attained by the paper. Enter yes, no, n/a, or an explanation if appropriate. Yes.*

Limitations *The authors are encouraged to create a separate "Limitations" section in their paper. The paper should point out any strong assumptions and how robust the results are to violations of these assumptions (e.g., independence assumptions, noiseless settings, model well-specification, asymptotic approximations only holding locally). Discussed in Section 9.*

Theory, Assumptions and Proofs *If you are including theoretical results, did you state the full set of assumptions of all theoretical results, and did you include complete proofs of all theoretical results? All assumptions should be clearly stated or referenced in the statement of any theorems. The proofs can either appear in the main paper or the supplemental material, but if they appear in the supplemental material, authors are encouraged to provide a short proof sketch to provide intuition. Enter yes, no, n/a, or an explanation if appropriate. Yes. Discussed in Section 5 and Appendix.*

Experimental Result Reproducibility *If the contribution is a dataset or model, what steps did you take to make your results reproducible or verifiable? Depending on the contribution, reproducibility can be accomplished in various ways. For example, if the contribution is a novel architecture, describing the architecture fully might suffice, or if the contribution is a specific model and empirical evaluation, it may be necessary to either make it possible for others to replicate the model with the same dataset, or provide access to the model. In general, releasing code and data is often one good way to accomplish this, but reproducibility can also be provided via detailed instructions for how to replicate the results, access to a hosted model (e.g., in the case of a large language model), release of a model checkpoint, or other means that are appropriate to your research. Enter yes, no, n/a, or an explanation if appropriate. Yes. Discussed in Sections 6, 4 and F.*

Open Access to Data and Code *If you ran experiments, did you include the code, data, and instructions needed to reproduce the main experimental results (either in the supplemental material or as a URL)? Please see the NeurIPS code and data submission guidelines for more details. While we encourage release of code and data, we understand that this might not be possible, so no is an acceptable answer. Papers cannot be rejected simply for not including code, unless this is central to the contribution (e.g., for a new open-source benchmark). At submission time, to preserve anonymity, remember to release anonymized versions. Enter yes, no, n/a, or an explanation if appropriate. Yes. Discussed in Sections 6, 4 and F.*

Experimental Setting/ Details *If you ran experiments, did you specify all the training details (e.g., data splits, hyperparameters, how they were chosen)? The full details can be provided with the code, but the important details should be in the main paper, and information about how hyperparameters were selected should appear either in the paper or supplementary materials. Enter yes, no, n/a, or an explanation if appropriate. Yes, in Sections 6 and F.*

Experiment Statistical Significance *Does the paper report error bars suitably and correctly defined or other appropriate information about the statistical significance of the experiments? Yes, results are averaged over 3 seeds and the standard deviation is reported.*

Experiments Compute Resource *For each experiment, does the paper provide sufficient information on the computer resources (type of compute workers, memory, time of execution) needed to reproduce the experiments? Yes.*

Code Of Ethics *Have you read the NeurIPS Code of Ethics and ensured that your research conforms to it? Enter yes, no, or an explanation if appropriate. Yes.*

Broader Impacts *If appropriate for the scope and focus of your paper, did you discuss potential negative societal impacts of your work? Please see the Paper Checklist Guidelines for detailed instructions and examples of points that you may choose to discuss. Enter yes, no, n/a, or an explanation if appropriate. Yes, in Section A.*

Safeguards *Do you have safeguards in place for responsible release of models with a high risk for misuse (e.g., pretrained language models)? Released models that have a high risk for misuse or dual-use should be released with necessary safeguards to allow for controlled use of the model, for example by requiring that users adhere to usage guidelines or restrictions to access the model. Enter yes, no, n/a, or an explanation if appropriate. N/A.*

Licenses *If you are using existing assets (e.g., code, data, models), did you cite the creators and respect the license and terms of use? Cite the original paper that produced the code package or dataset. If possible, include a URL. Be sure to check the original license and respect its conditions. Enter yes, no, n/a, or an explanation if appropriate. Yes, in Section 4 and Section F.*

Assets *If you are releasing new assets, did you document them and provide these details alongside the assets? Researchers should communicate the details of the dataset or the model as part of their submissions via structured templates. This includes details about training, license, limitations, etc. Enter yes, no, n/a, or an explanation if appropriate. Yes, an anonymized version of the code has been shared.*

Crowdsourcing and Research with Human Subjects *If you used crowdsourcing or conducted research with human subjects, did you include the full text of instructions given to participants and screenshots, if applicable, as well as details about compensation (if any)? Including this information in the supplemental material is fine, but if the main contribution of your paper involves human subjects, then we strongly encourage you to include as much detail as possible in the main paper. According to the NeurIPS Code of Ethics, you must pay workers involved in data collection, curation, or other labor at least the minimum wage in your country. Enter yes, no, n/a, or an explanation if appropriate. N/A.*

IRB Approvals *Did you describe any potential participant risks and obtain Institutional Review Board (IRB) approvals (or an equivalent approval/review based on the requirements of your institution), if applicable? Depending on the country in which research is conducted, IRB approval (or equivalent) may be required for any human subjects research. If you obtained IRB approval, you should clearly state this in the paper. For initial submissions, do not include any information that would break anonymity, such as the institution conducting the review. Enter yes, no, n/a, or an explanation if appropriate. N/A.*